Nanofiltration Membranes with Crumpled Polyamide Films: A Critical Review on Mechanisms, Performances, and Environmental Applications

Senlin Shao[a], Fanxi Zeng[a], Li Long[c], Xuewu Zhu[b], Lu Elfa Peng[c], Fei Wang[c], Zhe Yang[c*], and Chuyang Y. Tang[c*]

[a] School of Civil Engineering, Wuhan University, 430072, PR China

[b] School of Municipal and Environmental Engineering, Shandong Jianzhu University, Jinan, 250101, PR China

[c] Department of Civil Engineering, the University of Hong Kong, Pokfulam, Hong Kong, SAR, China

CORRESPONDING AUTHORS

Zhe Yang - Department of Civil Engineering, The University of Hong Kong, Hong Kong 999077, P. R. China; https://orcid.org/0000-0003-0753-3902; Tel: +852-2857 8470; E-mail address: zheyang@connect.hku.hk

Chuyang Tang - Department of Civil Engineering, The University of Hong Kong, Hong Kong 999077, P. R. China; https://orcid.org/0000-0002-7932-6462; Tel: +852 28591976; E-mail: tangc@hku.hk

AUTHORS

Senlin Shao - School of Civil Engineering, Wuhan University, 430072, PR China; https://orcid.org/0000-0003-0953-5151.

Fanxi Zeng - School of Civil Engineering, Wuhan University, 430072, PR China.

Li Long - Department of Civil Engineering, The University of Hong Kong, Hong Kong 999077, P. R. China; https://orcid.org/0000-0002-7951-3276.

Xuewu Zhu - School of Municipal and Environmental Engineering, Shandong Jianzhu University, Jinan, 250101, PR China

Lu Elfa Peng - Department of Civil Engineering, The University of Hong Kong, Hong Kong 999077, P. R. China; https://orcid.org/0000-0002-3223-4608.

Fei Wang - Department of Civil Engineering, The University of Hong Kong, Hong Kong 999077, P. R. China.

NOTES

The authors declare no competing financial interest.

TOC

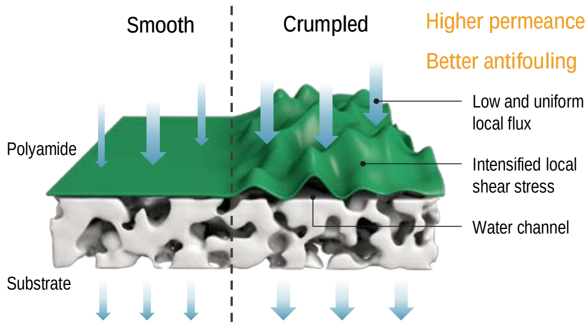

Smooth
Crumpled
Higher permeance
Better antifouling
Low and uniform local flux
Polyamide
Intensified local shear stress
Water channel
Substrate

■ ABSTRACT

Nanofiltration (NF) membranes have been widely applied in many important environmental applications including water softening, surface/ground water purification, wastewater treatment, and water reuse. In recent years, a new class of piperazine (PIP)-based NF membranes featuring a crumpled polyamide layer has received considerable attention due to their great potential for achieving dramatic improvements in membrane separation performance. Since the report of novel crumpled Turing structures that exhibited an order magnitude enhancement in water permeance (*Science* 360(6388), 518-521, 2018), the number of published research papers on this emerging topic has grown exponentially to approximately 200. In this critical review, we provide a systematic framework to classify the crumpled NF morphologies. The fundamental mechanisms and fabrication methods involved in the formation of these crumpled morphologies are summarized. We then discuss the transport of water and solutes in crumpled NF membranes and how these transport phenomena could simultaneously improve membrane water permeance, selectivity, and anti-fouling performance. The environmental applications of these emerging NF membranes are highlighted, and future research opportunities/needs are identified. The fundamental insights in this review provide critical guidance on the further development of high-performance NF membranes tailored for a wide range of environmental applications.

Keywords: Nanofiltration, Polyamide, Crumpled morphology, Water transport pathway, Selectivity, Membrane fouling

Synopsis: Nanofiltration membranes with well-controlled morphologies have the potential to simultaneously improve water permeance, selectivity, and anti-fouling ability.

■ INTRODUCTION

Nanofiltration (NF) is a pressure-driven membrane process that has separation abilities between ultrafiltration (UF) and reverse osmosis (RO). A typical NF membrane has a molecular weight cut-off between 150 and 2000 Da and is efficient in rejecting multivalent ions and organic compounds.[1, 2] Therefore, NF technology has been widely adopted in drinking water purification,[3] wastewater reclamation,[4, 5] water softening,[3, 6] food processing,[7] pharmaceutical industry,[8] etc. Unlike seawater, the feed water in these applications generally has relatively low osmotic pressures; thus, increasing the permeance of NF membranes could significantly improve water production and reduce energy consumption.[9, 10] However, membrane separation performance is constrained by the permeance -selectivity tradeoff: highly permeable membranes typically have low rejections to target substances and vice versa.[11-14] Consequently, it is a major challenge to improve the permeance of NF membrane without compromising selectivity.

Currently, the gold standard for commercially available NF membranes is thin-film composite (TFC) polyamide membranes, which are composed of a polyamide rejection layer, a UF substrate, and a non-woven fabric support.[15-17] The polyamide rejection layers of NF membranes are often prepared by interfacial polymerization, with piperazine (PIP) and trimesoyl chloride (TMC) as the most used monomers.[13, 15, 16] It should be noted that the NF membrane in this review, thus, specifically refers to the TFC polyamide membrane prepared using interfacial polymerization reaction with PIP and TMC. With numerous in-depth studies on the polyamide selective layer formed by the interfacial polymerization reaction, the morphology of the polyamide layer is found to have a significant influence on the permeance of TFC membranes. For example, in RO membranes formed by *m*-phenylenediamine (MPD) and TMC (Fig. 1a), the "ridge-and-valley" morphology of the formed polyamide layer greatly improves the permeance of RO membrane by increasing the effective filtration area[18-20] and creating voids in the polyamide layer,[18, 20-25] whose self-guttering effect further improves membrane permeance.[20, 26-28] Unlike RO membranes, commercially available NF membranes formed by PIP and TMC are relatively smooth (Fig. 1a). Inspired by the highly efficient water transport in TFC RO membranes,[18, 19] one may wonder if NF membranes with crumpled polyamide layers may effectively enhance water permeance over their smooth counterparts to overcome the permeance -selectivity tradeoff.

In recent years, PIP-based NF membranes with crumpled polyamide layers have received considerable attention (Fig. 1b). Particularly followed by the seminal work of Turing structure in *Science* in 2018,[29] the number of publications on crumpled NF membranes is rapidly growing. Researchers have developed various methods to fabricate NF membranes with different surface morphologies (Table S1), along with major enhancement of water permeance from ~10 to >20 LMH/bar, pushing the separation performance (e.g., water-Na_2SO_4 selectivity (A/B) vs. water permeance (A)) towards the top right corner in the upper bound diagram (Fig. 1c). Despite such promising progress in crumple NF membranes, a dedicated review on the formation of and transport of this emerging type of membranes is not yet available. More importantly, the underlying mechanisms (e.g., how the crumpled morphologies affect the transport of water and solutes) have yet to be systematically examined. In addition, the related fouling behavior of crumpled NF membranes has not been fully understood.

Therefore, to better facilitate the in-depth understanding of crumped NF membranes, this critical review summarizes their recent progress, with particular emphasis on 1) a systematic framework to classify the crumpled NF morphologies, 2) fundamental mechanisms and fabrication methods involved in the formation of these crumpled morphologies, 3) transport mechanisms of water and solutes in crumpled NF membranes, and 4) fouling propensities of crumpled NF membranes. The critical insights and important design criteria gained in this review facilitate the development of more efficient environmental applications with high energy efficiency and/or better anti-fouling properties. This review also identifies the critical research gaps and research opportunities pertaining to the further development of crumpled NF membrane.

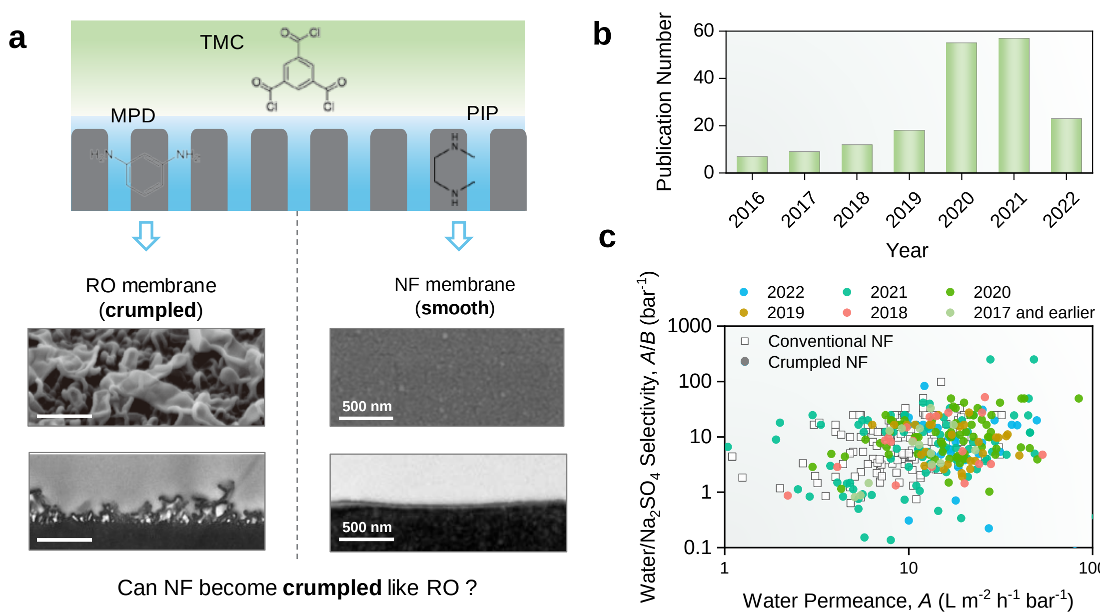

Figure 1. (a) Typical morphologies of polyamide layer of RO membrane (ESPA3, formed by MPD and TMC) and NF membrane (NF270, formed by PIP and TMC).[30] (b) Number of peer-reviewed publications on PIP-based NF membranes with crumpled morphologies (incomplete data for the Year 2022). (c) Water/Na_2SO_4 selectivity (A/B) vs. water permeance (A) for PIP-based NF membranes with crumpled morphologies (detailed data are provided in Table S1).

Open dots indicate conventional NF membranes with smooth polyamide layers, and closed dots indicate novel NF membranes with crumpled polyamide layers; the data of crumpled NF are color-mapped based on their published years. The scanning electron microscopy (SEM) images were modified from the previous study[30] with copyright permission.

■ CLASSIFICATION OF CRUMPLED MORPHOLOGIES, THEIR FORMATION MECHANISMS, AND FABRICATION METHODS

Typical Crumpled Morphology of NF Membranes and Their Separation Performance

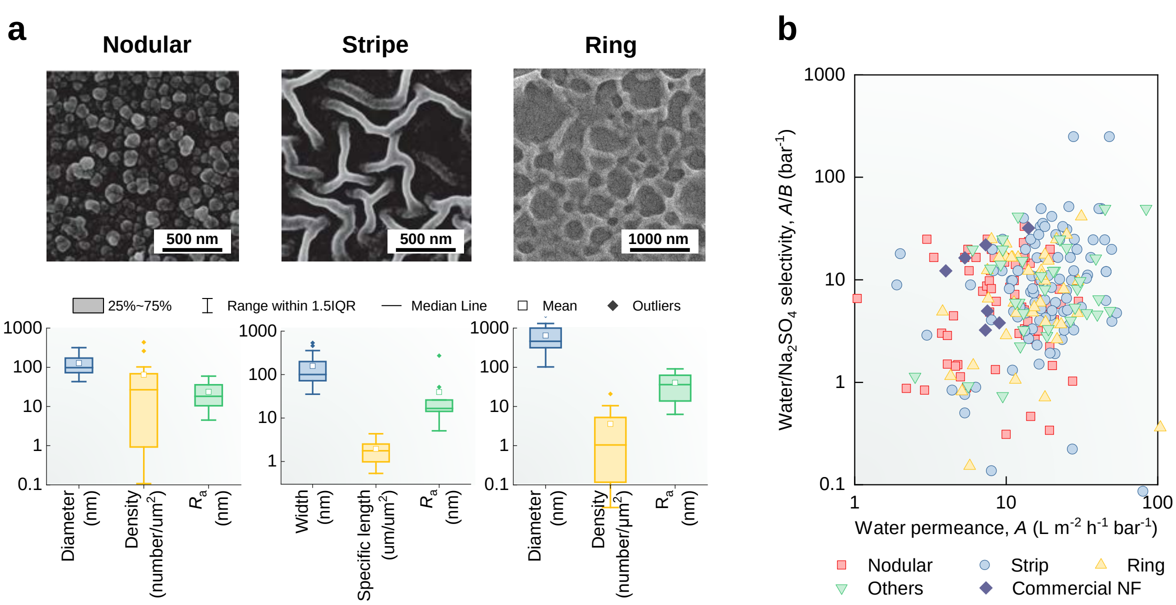

Figure 2. Classification of crumpled morphologies (a) and their corresponding separation performances (b). Diameter, width, and density (number density for nodular and ring structures, and specific length for stripe structure) of the morphologies were based on the statistics of the SEM images of the previous studies (Table S3); Average roughness (R_a) was based on the atomic force microscope (AFM) results of the previous studies. Separation performances of commercial

NF are provided in Table S4. The SEM images were modified from the previous studies[29, 31] with copyright permission.

Table S1 summarizes crumpled polyamide layers for PIP-based NF membranes reported in previous studies. Specifically, nodular,[29, 32] stripe,[29, 33, 34] and ring[31, 35-37] structures are the three most common morphologies (Fig. 2). Other structures, such as fishnet-like and octopus sucker-like structures,[38, 39] are occasionally represented in some studies (Fig. S1 provides the SEM images of some examples). Among these morphologies, only the nodular structure is observed in existing commercial membranes,[40] and other morphologies mostly exist in custom-fabricated membranes in literature papers.

In terms of the nodular structure (Fig. 2a), its diameter is often in the range of 50 to 300 nm, with a typical areal number density ranging from 5 to 300 per μm^2. Based on a limited number of TEM studies,[29, 32, 41-45] the nodular generally has arc-shaped cross-sections, and the ratio of height to diameter is mostly lower than 1. Possibly because of this low ratio, the average roughness (R_a) obtained using atomic force microscopes (AFM) is often in the range of 10 to 50 nm. In terms of stripe structure, the width of the stripes generally ranges from 50 to 400 nm, and the specific length (length/area) ranges from 500-5000 nm per μm. Like the nodular structure, the stripe structures also have low heights,[29, 46-49] which is also evidenced by the low R_a (5-50 nm). Some ring structures are possibly formed by the collapse of canopy structures or large nodular structures.[50, 51] Therefore, its diameter can reach several μm, while its density is much lower than a typical nodular structure.

NF membranes with crumpled morphologies often exhibit better separation performance in terms of water permeance and water/solute selectivity than commercially available NF membranes (Fig. 2b). Among the common morphologies, the stripe structure appears to be more promising compared with nodular and ring structures. The associated transport mechanisms in crumpled NF membranes will be further discussed under the section "Critical Analysis of Water and Solutes Transport Mechanisms for Crumpled NF Membranes".

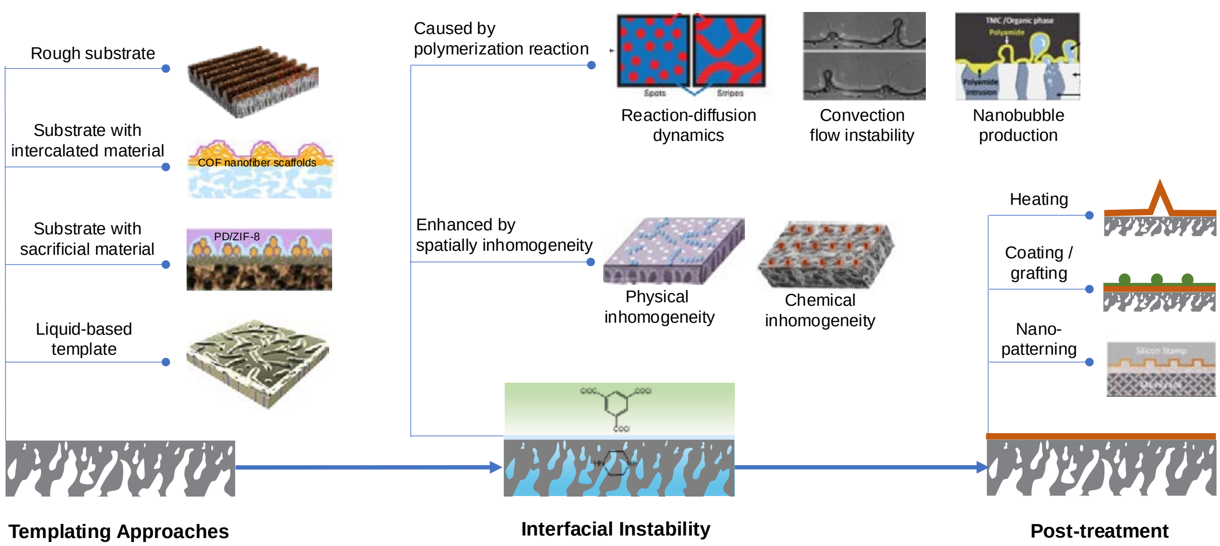

Figure 3 Formation of crumpled morphologies of polyamide layers. Templating approach, interfacial instability regulating, and post-treatment could be used before, during, and after the formation of polyamide layers, respectively. The images were modified from the previous studies with copyright permission (rough substate,[52] substrate with intercalated material,[53] substrate with sacrificial material,[54] liquid-based template,[55] reaction-diffusion dynamics,[29] convection flow instability,[56] nanobubble production,[26] physical inhomogeneity,[57] nano-patterning[58]).

Mechanisms and Fabrication Methods for Crumpled Morphology of Polyamide Layer

The PIP-based polyamide layer on support substrates (e.g., polysulfone membrane) is generally formed through interfacial polymerization of PIP and TMC monomers.[15, 16, 19] During interfacial polymerization, the substrate is first wetted by a PIP aqueous solution, then immersed in a TMC organic solution. PIP and TMC can react at the aqueous/organic interface and form a polyamide film on the substrate. Post-treatments, such as heating and drying, are often applied to stabilize the polyamide film and further adjust its properties. Based on the protocols of interfacial polymerization, the following strategies could be used to fabricate a crumpled polyamide layer (Fig. 3): 1) using templating approaches to create a rough aqueous/organic interface for interfacial polymerization, so that the formed polyamide film achieves a rough morphology following the aqueous/organic interface; 2) regulating and intensifying the interfacial instability during the reaction of interfacial polymerization; 3) post-processing the formed polyamide layer.

Templating Approaches. A rough templating substrate can directly lead to an uneven aqueous/organic interface on the surface of the substrate. Considering the typical thickness of tens of nm for PIP-based polyamide layers,[59-61] the feature size of the templating substrate should be in the range of hundreds of nm to several μm to affect the formation of polyamide rejection layers. While the typically used polysulfone substrate is relatively smooth,[20, 62] a few strategies are available to prepare a rough templating substrate. One strategy is patterned membranes. Patterned membranes, often reported for fouling control,[63-65] typically involve fabrication methods such as phase separation micro-molding,[66, 67] thermal embossing/nanoimprinting[65, 68, 69], and 3D printing.[70, 71] Previous studies have constructed patterns such as grooved lines,[64, 72, 73] pillars,[74] prism,[66] pyramid[75] with dimensions ranging from tens of nm to hundreds of μm. These patterned membranes, when used as substrates, are expected to create aqueous/organic interfaces with regular/periodical morphological features. A second strategy involves the use of scaffolds with rough surfaces, such as non-woven fabrics, stainless steel meshes,[76] and microfiltration membranes with large pores.[77, 78] Unlike a patterned substrate, these rough scaffolds usually have an irregular surface morphology. One critical challenge involved in using rough substrates is the increased risks of defect formation in the resulting polyamide rejection layers. For example, if directly conducting interfacial polymerization on rough scaffolds with large pores, the unsupported polyamide film formed over the macropores of the scaffolds is easily broken.[79, 80] This issue could be potentially addressed by plugging the macropores of the scaffolds with materials of desirable mechanical strength, water permeance, and adhesion force with the scaffold. Some examples include porous protein assemblies[78] and crosslinked polyvinyl alcohol (PVA).[76] To achieve a crumpled polyamide layer over the templating substrate, another key consideration is the fidelity of the rough morphology after the interfacial polymerization. Some studies suggested that the fidelity could be improved by decreasing monomer concentrations[72] and using a layered interfacial polymerization technique.[74, 81]

Even with a smooth substrate, one can deposit nanomaterials on its surface to create a rough aqueous/organic interface. Previous studies have deposited nanoparticles[57, 82-84] and nanofibers,[53] etc., on substrate surfaces. Common methods for nanomaterial deposition include vacuum filtration,[45, 54, 85, 86] spraying,[87, 88] in-situ growth,[47, 89-92] etc. An ideal deposition is a single layer of nanomaterials with a suitable distance between the individual particles/fibers. The size of nanomaterials may have a major influence: small sizes may minimize the change in morphologies, while large sizes may heighten the risk of defects.[84] In general, hydrophilic nanomaterials are recommended because they may induce the formation of nanochannels at the interface between the nanomaterial surface and the polyamide matrix.[93] For the nanomaterial-based templating approach, the key is to uniformly deposit nanomaterials without aggregation and stacking.[57] In addition, because the nanomaterial is often water impermeable, the intercalated materials may block the water flow through the resulting NF membrane, causing a compromise in water permeance. The adoption of porous materials, such as porous silica particles,[94] metal-organic frameworks,[82, 85, 95] covalent organic frameworks,[50, 96, 97] and molecular sieves,[87, 98, 99] may partially address this issue.

To minimize the impact of intercalated nanomaterials on the performance of NF, one can also use sacrificial materials, such as dissolvable nanoparticles[54, 100] and salt crystal[101, 102], which are readily removed after interfacial polymerization (e.g., by dissolving in water or acid). The removal of these sacrificial materials can create nanovoids in polyamide layers, which can effectively improve the permeance of NF membranes. For example, etching copper nanoparticles using 1% HNO_3 from a copper embedded NF membrane led to quadrupled water flux.[103]

In addition to solid templates, liquid-based templates may also be used under appropriate interfacial conditions.[55, 104] For example, to achieve an aqueous template, one could first leave a certain amount of water spread on the substrate surface by tuning rolling pressures and drying conditions. Under specific interfacial tensions, which are adjusted by adding surfactant into aqueous solution and using hydrophilic substrate (including surface-modified and interlayered membrane), the remaining water may form an uneven aqueous/organic interface on the substrate,[55, 105, 106] resulting in a crumpled polyamide layer after interfacial polymerization.

Interfacial Instability. The interfacial polymerization reaction is inherently associated with instability, which could be utilized to facilitate the formation of crumpled polyamide films. In fact, the interfacial instability is the key to the "ridge-and-valley" morphology of MPD-based polyamide layers.[19, 107] Currently, the interfacial instability during interfacial polymerization is mostly explained by the following three mechanisms:

1) Reaction-diffusion dynamics.[29, 108, 109] As one of the most famous models of reaction-diffusion dynamics, the activator-inhibitor model is often used to explain the formation of patterns.[110] In this model, the activator promotes the synthesis of itself and the inhibitor, while the inhibitor restricts the production of the activator.[110] If the diffusion speed of the inhibitor is faster than that of the activator ("local activation and lateral inhibition" proposal), periodic patterns such as spots and stripes (i.e., Turing patterns) may be formed. During the reaction of interfacial polymerization, amine monomers in the aqueous phase firstly diffuse to the organic phase and then react with acyl chloride monomers to form a polyamide film.[19] The amine monomer can be regarded as the activator because its diffusion causes the reaction, and the formed polyamide layer can be regarded as the inhibitor because of its self-limiting effect.[29]
2) Convection flow instability.[56, 111] Interfacial polymerization causes the consumption of monomers and the release of heat, leading to concentration and thermal gradients near the aqueous/organic interface, consequently density gradients and spatially varied interfacial tensions. The density gradient may cause Rayleigh–Bénard convection because gravity tries to pull down the denser liquid.[112] The spatially varied interfacial tension may also lead to Marangoni convection because the liquid tends to flow to the place of lower surface

tension.[112] During interfacial polymerization, these convection flows may result in a fluctuating interface, which might be responsible for the formation of the crumpled polyamide.

3) Nanobubble formation. Some recent literature suggested that the crumpled morphology of polyamide layers could be formed by interfacial degassing.[113-116] That is, the interfacial reaction between amine and acyl chloride monomers could generate both heat and H^+, which favors the conversion of dissolved HCO_3^- in the aqueous phase (alkaline solution) to release CO_2 nanobubbles. By the confinement of porous substrate, these nanobubbles tend to deliver amine monomers to the reaction front due to the convention under a pressure gradient. In addition, these degassed bubbles could be encapsulated by the nanofilm to tune the polyamide morphology.

Based on these mechanisms, to enhance the interfacial instability, one could increase the formation of polyamide (inhibitor), enhance thermal and concentration gradients, and/or intensify heat and H^+ release. Increasing the reaction rate can well-match these goals, e.g., by adding acid acceptor,[114, 117] increasing reaction temperature,[31, 118] and adding other co-monomers.[119] One can also control the diffusion of PIP (activator) and change the interfacial tension by adding chemicals such as PVA,[29] salts,[120, 121] and surfactants[34, 122] to the PIP solution, and coating a hydrophilic gel layer on the substrate.[123]

The interfacial instability of interfacial polymerization can be enhanced by the spatial inhomogeneity of the reaction. Physical inhomogeneity (i.e., inhomogeneity in monomer storage) of the reaction could be readily achieved using rough substrates (see the section "Templating

Approaches"). For example, the valleys of a rough surface may have more PIP monomer storages, and consequently may lead to more violent reactions.[26, 79, 124] Chemical inhomogeneity could be achieved using a substrate with reactive spots,[125-128] and the inhomogeneity may be increased because of the reaction of TMC with these reactive spots. Many studies[45, 46, 84, 106, 129, 130] reported that the addition of nanomaterial in PIP solution could lead to a crumpled polyamide layer. A possible explanation for this phenomenon is that these nanomaterials intensify the inhomogeneity of the interfacial polymerization, both physically and chemically.[96, 131, 132]

Post-treatment. Post-treatment is an important step in improving the stability and performance of the NF membrane. Because the polyamide layer may have different thermal expansion and contraction coefficients compared with the substrate, a heating post-treatment may lead to delamination and buckling of the polyamide layer at the micro-/nano-scale,[108] resulting in a rough morphology.[133, 134] Additionally, surface coating and grafting sometimes cause a rough morphology by adding an additional layer or changing the properties of polyamide layers.[135-139] Patterning methods can also be used in the post-treatment of the polyamide layer. Because of the thin thickness of the polyamide layer,[59-61] the dimension of the pattern is generally tens of nm, and previous studies generally used nanoimprinting method.[58, 68, 140, 141] After the nanoimprinting of commercial NF membranes, their anti-fouling performances are significantly improved (see the section "Critical Analysis of Fouling Propensities of Crumpled NF Membranes").

Among the various strategies for the fabrication of crumpled NF membranes, templating approaches can achieve the morphology of a polyamide layer similar to that of the templating substrate, except that the aqueous and nanomaterials-based templating may lead to a stripe morphology after the collapse of the polyamide layer.[55, 84, 142] By regulating the interfacial instability, the polyamide layer is most likely to form periodic nodular and stripes. With post-processing, especially the patterning method, the polyamide morphology can be further regularized and customized. Although most of the strategies are in the laboratory stage, some of them show the potential for scale-up, with small changes to the existing processing line for interfacial polymerization. For example, by adding a rinsing process to create a PVA interlayer on the substrate, a pilot-scale production line for NF with periodic stripes was successfully established.[105] Additionally, templating approach, interfacial instability regulating, and post-processing are at different steps of the production line, and thus the three methods can be combined to further improve the performance of NF.

■ CRITICAL ANALYSIS OF WATER AND SOLUTES TRANSPORT MECHANISMS FOR CRUMPLED NF MEMBRANES

Compared to their conventional (smooth) counterparts, TFC NF membranes with crumpled morphologies could have many advantages, including enhanced water permeance and possibly enhanced water/solute and solute/solute selectivity (Fig. 1). Therefore, this section critically analyzes the underlying mechanisms responsible for the improved separation performance with the assistance of conceptual models and literature surveys.

Mechanisms Responsible for Enhanced Water Permeance with Crumpled Morphologies

Several mechanisms can be applied to explain the enhanced water permeance of crumpled NF membranes,[29, 55, 113] such as an increased effective surface area for filtration, decreased thickness of the polyamide layer, and optimized water transport pathways (Fig. 4).

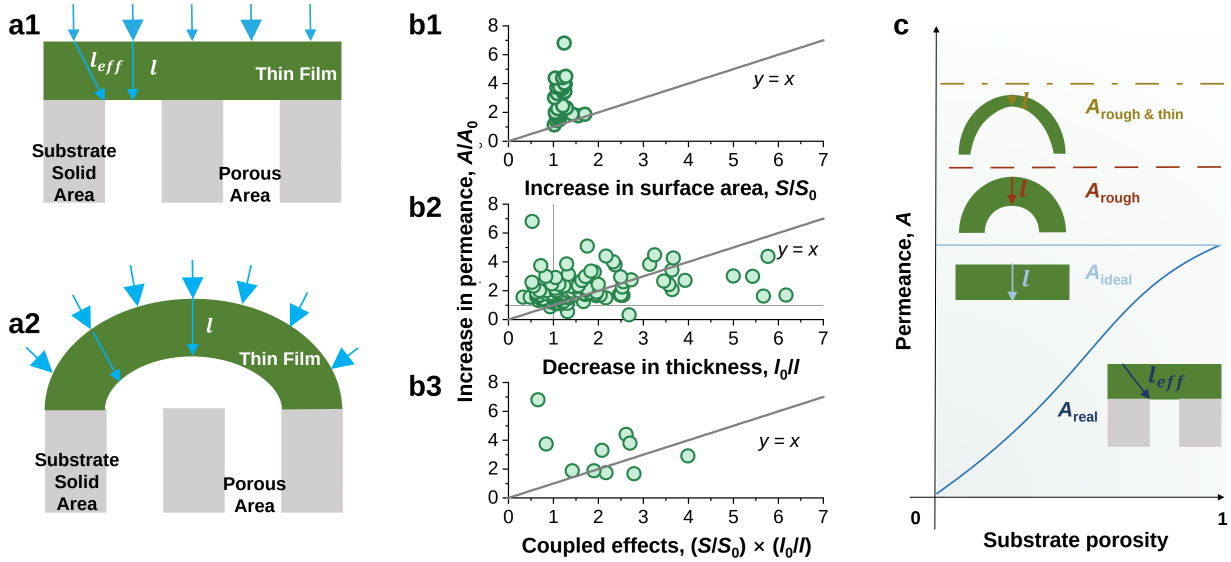

Figure 4. Conceptual models (a) for elucidating the mechanisms of enhanced water permeance of crumpled TFC membranes, where l_{eff} is defined as the actual (effective) water transport pathways, and l is the intrinsic thickness of the polyamide rejection layer (i.e., the ideal water transport pathway). (b) Analysis of literature data of crumpled NF membranes in Table S1 with respect to the effect of surface area ratio (S/S_0), thickness reduction ratio (l_0/l), and their coupled effects [$(S/S_0) \times (l_0/l)$] on water permeance enhancement. The line of function $y = x$ was superimposed in each sub-figure. The conceptual model (c) further highlights the benefits of 1) altered transport path (A_{ideal}) with the increased substrate porosity; 2) increased surface area (A_{rough}, the superimposed red line); and 3) together with the reduced thickness of the crumpled polyamide layer ($A_{rough\ \&\ thin}$, the superimposed yellow line). Figures a and c were modified from the previous study[26] with copyright permission.

Increased Surface Area of Polyamide Layers. An intuitive understanding of a crumpled membrane is that the surface area for water transportation could be significantly enhanced. For example, the striped membrane morphologies (assuming the half-cylinder shape), regardless of the thickness of the polyamide rejection layer, could have the theoretical water permeance enhancement factor of 1.57 (Fig. S2a). For a hemispherical shape of nodular morphology, the theoretical membrane surface area enhancement factor could be two compared to a smooth counterpart (Fig. S2b), potentially translating into doubled water permeance. Although the current literature reports that the characteristic heights of crumpled morphologies are generally low (Fig. 2), crumpled morphologies with higher characteristic heights could result in much higher increases in surface area. However, crumpled morphologies with higher characteristic heights may face the collapse of polyamide film.[20, 55] Future studies need to explore such phenomena to achieve a compromise between an enhanced surface area of polyamide and its mechanical stability.

We further performed a comparison between membrane water permeance enhancement and membrane surface area enhancement (characterized by AFM) based on a literature survey (Fig. 4b1). These results further corroborate the importance of the increased surface area of crumpled polyamide layers in improving membrane water permeance. It is interesting to note that the increase in membrane surface area alone is not enough to explain the significant flux enhancement observed in the literature. In our analysis, most of the experimental data points are above the theoretical line based on enhanced surface area (i.e., $y = x$), which implies that additional mechanisms may also play important roles.[29, 55, 113]

Decreased Thickness of Polyamide Layers. In addition to increased membrane surface area, the formation of crumpled morphology is often accompanied by the reduced intrinsic thickness of polyamide layers (Fig. 4b2),[122, 143-149] which is possibly ascribed to the changes in interfacial polymerization reaction (see the section "Interfacial Instability") such as inhibited amine monomer diffusion and facilitated polyamide film formation. This reduced thickness of the rejection layer, in some cases up to ~ 6 times, also favors improved water permeance of crumpled NF membranes (Fig. 4b2). Interestingly, the decreased polyamide thickness, often accompanied by the enhanced surface area ratio, could have a synergistic effect on membrane water permeance enhancement, which might explain the close to one order of magnitude enhancement of water permeance for crumpled NF membranes (Fig. 4b3).

Optimized Water Transport Pathways. Compared to the mechanisms of enhanced surface area and reduced thickness of polyamide layers, the mechanism of optimized water transport pathways for crumpled NF membranes has been far less discussed in the literature. Indeed, for the conventional TFC membranes, its separation performance can be severely constrained by the funnel effect,[26, 150-152] which is often ascribed to the low porosity of the substrate (typically below 10%).[153] As illustrated in Fig. 4a1, the water transport distance away from the substrate pore (l_{eff}) of conventional smooth TFC membrane is significantly greater than the thickness of its polyamide rejection layer (l), resulting in significantly higher hydraulic resistance and hence lower water permeance compared to a free-standing polyamide film (an ideal case). To overcome the funnel effect, the crumpled polyamide layer of NF membranes, containing voids that span over multiple substrate pores (Fig. 4a2), could potentially shorten the water transport distance in the rejection layer (in a fashion similar to the inclusion of a high-permeance gutter layer[151, 154, 155]). This effect, coined as the self-gutter effect by Tang and coworkers,[9] can greatly reduce the hydraulic resistance by effectively shortening the water transport pathways (close to the intrinsic thickness of the rejection layer, Fig. 4a2).

To deepen the understanding of this mechanism, Fig. 4c presents the conceptual model of optimized water transport pathways for improving water permeance. The dark blue line represents the actual membrane water permeance (A_{real}), whereas the light blue line represents the ideal water permeance (free-standing polyamide film, A_{ideal}), with the varying substrates porosities. Due to the funnel effect, the actual water transport distance (l_{eff}) of a conventional TFC NF membrane is significantly longer than the ideal transport distance (l) of a free-standing polyamide film. With the lower substrate porosity, the funnel effect is more severe, resulting in significantly lower water permeance. The crumpled polyamide morphologies, equivalent to the effect of the increasing substrate porosity of a flat polyamide rejection layer, could significantly improve membrane water permeance thanks to the greatly shortened water transport pathways, which approach the ideal water permeance (light blue line). Alternatively, the effect of the nanovoids within the crumpled polyamide rejection layer could be interpreted through their self-gutter effect on shortening the transport path to approach the ideal water permeance.[9, 28] It is also interesting to note that, as an added advantage, the altered water transport pathways tend to result in more uniform flux distribution, which is beneficial to reducing fouling tendency by decreasing the accumulation of foulants in the localized hot spot zone[151, 156] (see the section "Crumpled Polyamide Film and Local Flux").

We further benchmark the theoretical water permeance of the rough NF membrane with an ideal rejection layer (without the effect of substrate, superimposed in red color in Fig. 4c), which could even successfully exceed the ideal water permeance of the smooth NF membrane due to the additional benefit of increased filtration area. In reality, a crumpled NF membrane could simultaneously achieve a reduced thickness of the polyamide layer in addition to optimized water transport pathways and increased surface areas (line in yellow color, Fig. 4c), resulting in the greatest water permeance thanks to these synergistic effects. Overall, our theoretical analysis is in good agreement with the literature results, where crumpled NF membranes showed up to an order of magnitude higher water permeance compared to the control.[96, 131, 157-160]

Mechanisms Responsible for Enhanced Water/solute and/or Solute/solute Separation of Crumpled Morphologies

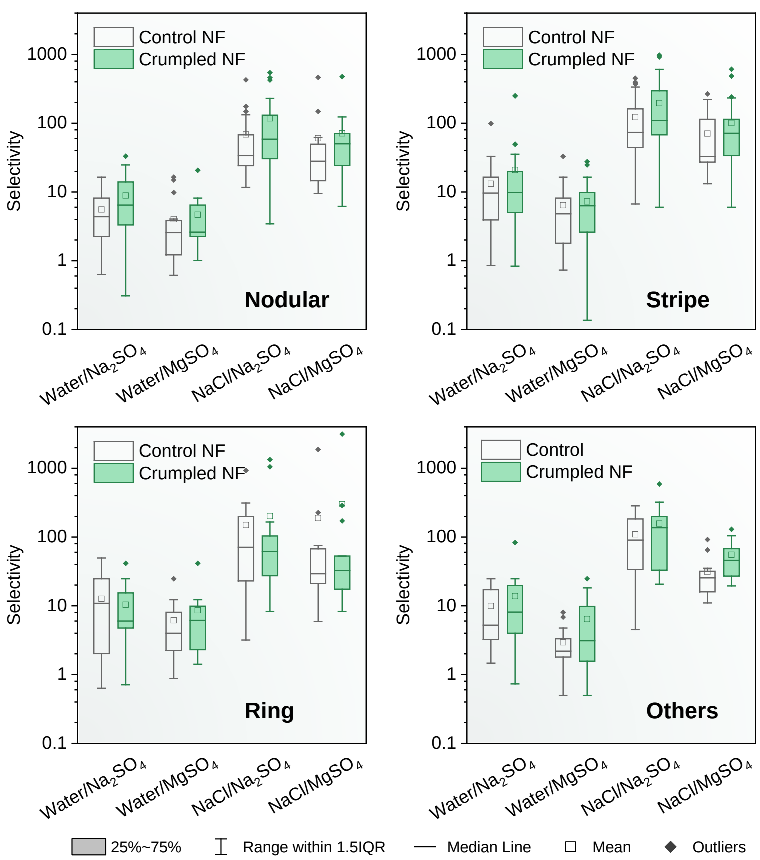

Figure 5. Water/Na_2SO_4, water/$MgSO_4$, NaCl/Na_2SO_4, and NaCl/ $MgSO_4$ selectivity of the PIP-based NF membranes with different crumpled morphologies. Detailed data of the box plots are shown in Table S2.

In addition to the water permeance enhancement, Fig. 5 shows that some crumpled NF membranes may offer enhanced water/solute and/or solute/solute selectivity (e.g., Water/Na_2SO_4, Water/$MgSO_4$, NaCl/Na_2SO_4, and NaCl/$MgSO_4$) thanks to the fine-tuned physicochemical properties of the crumpled polyamide layers. As discussed in the section "Interfacial Instability", the interfacial polymerization reaction rate could be greatly altered, which may further result in changes in membrane crosslinking degree and sometimes the optimized membrane pore size uniformity.[37, 96, 117, 136, 137, 161, 162] For instance, Liang et al.[34] applied sodium dodecyl sulfate (SDS) to manipulate the interfacial polymerization reaction between PIP and TMC, resulting in not only crumpled polyamide morphologies with enhanced water permeance but also more uniform pore size distribution. The resulting NF membrane showed enhanced selectivity towards a wide range of solutes, including mono/di-valent ions and neutral solutes. Interestingly, due to its relatively large pore size in the range of 1 – 2 nm,[163] the variation of pore size distribution is more effective in enhancing the rejection of divalent ions (e.g., SO_4^{2-}, Ba^{2+}, and Ca^{2+}) or other larger solutes (e.g., glucose and sucrose), and less pronounced in enhancing the rejection of monovalent ions (e.g., Li^+, Na^+, and K^+),[34, 125, 133, 164-168] and therefore improving its mono-/di-valent ions selectivity (e.g., NaCl/Na_2SO_4 and NaCl/$MgSO_4$ selectivity in Fig. 5).

It is also interesting to note that crumpled NF membranes could also generate localized turbulence to mitigate the localized concentration polarization effect,[169-171] which could potentially enhance the water/solute and solute/solute selectivity. Indeed, compared to the smooth counterparts, the crumpled/patterned polyamide films could enhance the localized mass transfer to improve the back diffusion of solute to the bulk,[169] thereby alleviating the concentration polarization and improving both membrane water flux and salt rejection.[170] For example, by comparing the fouling and rejection capability of the crumpled NF membrane with grooves-pattern in both parallel and perpendicular flow orientations, the reduced concentration polarization was revealed.[171] Nevertheless, a recent study conducted by Zhou et al.[172] suggested that crumpled morphology may increase the effect of concentration polarization effect, but this increase was compensated by the reduced local flux due to the increase in filtration area. These disparate observations might be partly attributed to the different roughness patterns involved, which calls for more future studies. Although few studies focus on the solute/solute selectivity induced by the mitigated concentration polarization effect of the crumpled membranes, different diffusion coefficients of various ions (e.g., the diffusion coefficient of Na^{+} is approximately twice that of Ca^{2+}) could lead to different concentration polarization mitigation degrees (different solutes rejection enhancement), which might result in the enhanced solute/solute selectivity.

It should also be noted that some fabrication procedures of crumpled polyamide layer may increase the risks of defect formation (e.g., templating approaches).[98, 173, 174] Additionally, the less-supported ridge of the crumpled layer may be vulnerable to external damage (e.g., high pressure).[55, 80] When defects are presented in a polyamide layer, although these defect spots can increase water permeance, it is often very risky to result in reduced water/solute and solute/solute selectivity. Future studies should make efforts to minimize defects in the polyamide layer during the fabrication of crumpled NF membranes.

■ CRITICAL ANALYSIS OF FOULING PROPENSITIES OF CRUMPLED NF MEMBRANES

Membrane fouling is a major obstacle to NF applications. Fouling can cause severe flux losses that need to be restored by physical/chemical cleaning. Fouling of NF membranes is often associated with the deposition of organic substances and the formation of biofilm on membrane surfaces,[175-177] which can be greatly influenced by foulant-membrane interactions and hydrodynamic conditions near the membrane surface.[178, 179] A crumpled membrane surface can affect both foulant-membrane interactions and hydrodynamic conditions, thus showing significant impacts on membrane fouling.

Surface Roughness and Foulant-membrane Interaction

A crumpled surface increases the roughness of a membrane. In the context of RO, since modern polyamide TFC RO membranes typically show a "ridge-and-valley" rough surface,[20, 60] researchers have long been focusing on the relationship between roughness and fouling from the perspective of foulant-membrane interaction. Elimelech and co-workers[180, 181] found that a polyamide membrane with high roughness had a more severe colloidal fouling (silica particles with 0.1 μm in diameter), because the colloids were preferentially deposited in the valleys of the membrane. In a follow-up paper, by analyzing the interaction between colloidal particles and membrane surface using Derjaguin-Landau-Verwey-Overbeek (DLVO) theory, these authors attributed the preferential colloidal deposition to the lower repulsive energy barrier at the valleys of the membrane surface.[182] Similar conclusion was also obtained by Bowen et al.,[183] who found much higher adhesion forces at the valleys of RO membranes using an AFM equipped with silica colloidal probes (4.2 μm). These pioneering studies imply that surface roughness increases the foulant-membrane interaction, especially in the valley region of a membrane, thereby increasing membrane fouling.

However, some recent studies suggest that enhanced foulant-membrane interactions only occur when the size/shape of the foulant and the valley are comparable (Fig. 6a). For example, Chuning et al.[179] found that the attachment of *S. epidermidis* cells (grape-like shape, ~1 μm in diameter) increased when the polyamide membrane surface became rougher, while that of *E. coli* cells (rod shape, ~3 μm in length) decreased. The authors attributed this result to the slightly smaller size of *S. epidermidis* than the size of valleys (0.5-3 μm), which enabled *S. epidermidis* to be trapped in these valleys. When the size of foulants is much smaller than that of the valley, the rough membrane "appears smooth" to such small-size foulant (Fig. 6b), and thus, the foulant-membrane interaction may be hardly affected by the roughness.[184, 185] Consistent with this, a recent study demonstrated that surface roughness had limited influence on the bovine serum albumin (BSA, ~7 nm) fouling for TFC membranes with well-controlled roughness.[186] When the size of foulants is larger than that of the valley, some studies suggested that the foulants-membrane interaction may be reduced by the decreased contact area.[74, 187, 188]

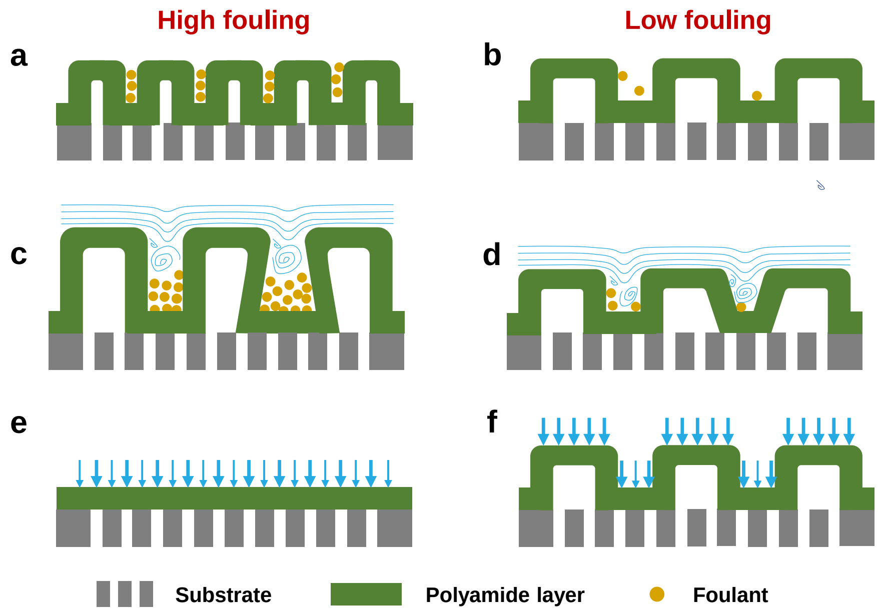

Figure 6. Crumpled morphologies of NF and membrane fouling. (a and b) Matched sizes between crumpled morphology and foulant may lead to more severe fouling. (c and d) Well-designed crumpled morphology can increase local shear stress. (e and f) Crumpled morphology can lead to a lower and more uniform local flux.

Surface Pattern and Local Shear Stress

A crumpled surface can disturb water flows and generate vortices (a similar fashion to fixed turbulence promoters), thereby enhancing local shear stress and reducing the deposition of foulants.[189, 190] For this reason, an important strategy to control membrane fouling is to introduce micro- or nano-patterns on membrane surfaces.[64] For example, a crumpled NF with well-defined patterned surfaces can be fabricated by using patterned substrates or post-nanoimprinting of the polyamide layer (see the sections “Templating Approaches” and “Post-treatment” for more details). Previous studies have constructed patterns such as grooved lines,[64, 72, 73] pillars,[74] prism,[66] pyramid[75] with dimensions ranging from tens of nm to hundreds of µm and revealed that these patterns could effectively reduce colloidal fouling,[75, 191] organic fouling,[68, 192, 193] and biofouling.[66 74] Through particle tracking techniques and computational fluid dynamics (CFD) modeling, several studies show that the ridges of the pattern have a higher shear stress[75, 194] and the valleys of the patterns can form vortexes.[194-196] As a result, a properly designed pattern can create favorable hydrodynamic environments to effectively mitigate foulant deposition.

Several points should be noted for more effectively increasing local shear stress with the surface patterns. First, hydraulic stagnant spots should be minimized. Surface patterns, while promoting localized turbulences, may also introduce some stagnant spots, especially at the shaded corners and deep valleys of crumpled surfaces (Fig. 6c). An important reason for the high fouling tendency of rough polyamide TFC RO membrane is the existence of some stagnant regions in their "ridge-and-valley" morphology.[179, 181] Second, well-designed topographies and dimension can achieve better anti-fouling properties.[67, 197, 198] For example, it was experimentally demonstrated that 45°-rotated pyramid patterns were more effective than pyramid and reverse-pyramid patterns in reducing particle deposition.[75] The sharkskin-mimetic pattern has an optimized space of 2 μm to mitigate biofouling[185, 199] with the prevention of biofilm by the enhancement of primary and secondary flow.[81, 200] Third, flow characteristics have important influences on the anti-fouling performance of patterns. In general, under a high crossflow velocity, large patterns are more effective than small ones for controlling particle deposition.[196] Additionally, fouling rates are lower when the flow direction is perpendicular to the lines of grooved patterns, while physical washes are more effective when the flow direction is parallel to the pattern lines.[191, 201] In addition to the well-defined patterns using the templating or post-nanoimprinting method, other fabrication methods may lead to random surface morphologies, as shown in Fig. 2, and the effect of these morphologies on the local shear stress needs to be further investigated.

Crumpled Polyamide Film and Local Flux

It is well accepted that membrane fouling is promoted at a higher flux because of 1) higher foulant loadings, 2) greater hydraulic drag on foulants, and 3) more severe concentration polarization.[178, 202] Membrane fouling rate is nearly zero when the flux is lower than a threshold value (i.e., critical flux),[203] and may exponentially increase with flux when it is higher than the threshold value.[204] In most scientific studies and practical applications, the generally mentioned "flux" is the macroscopically observed average flux of membrane coupons or membrane modules. However, the microscopic local flux, which is more closely related to fouling, could vary at the different locations of membranes.[151] For a membrane with non-uniform local flux, although the low-local-flux region has lower fouling, the high-local-flux region has much higher fouling due to the non-linear relationship between fouling rate and flux, and consequently the higher overall fouling.[205]

In a smooth polyamide layer, the hydraulic resistance is higher in the regions above substrate walls (because of the longer water transport pathway, Fig. 4a1), and that is lower in the region above the substrate pores.[206] Consequently, typically smooth NF membranes tend to have high non-uniformity of local flux, featuring much higher local flux over pore areas (Fig. 6e).[151, 156] Such non-uniform flux distribution could become even worse for substrates of lower porosities. When the polyamide layer becomes crumpled, the total filtration area increases (Fig. 4b). More importantly, the self-gutter effect leads to a more uniform local flux distribution (Fig. 6f), as experimentally confirmed through tracer filtration tests (e.g., using golden nanoparticles).[29, 151] With the lower and more uniform local flux, membrane fouling can be greatly reduced. This reason is regarded as the main driver for fouling reduction with crumpled membranes in some studies,[73] because of the huge impact of flux on membrane fouling.

In short, although a smooth polyamide film generally has a low fouling propensity, a crumpled polyamide film with well-designed morphologies could potentially out-perform its smooth counterpart as a result of the associated antifouling mechanisms such as the enhancement of local shear and the reduction of local flux. In addition to membrane fouling, inorganic scaling could also be influenced by surface morphologies.[207, 208] A rough surface often has a higher scaling potential, possibly because of the favorable formation/deposition of scaling nuclei at the valleys[209, 210] and the enhanced concentration polarization at the hydraulic stagnant spots.[172, 179] However, similar to membrane fouling, membrane scaling may also be mitigated by a well-designed crumpled morphology. For example, with a crumpled polyamide, the enhancement of local shear and the reduction of local flux may promote the detachment of scaling nuclei and crystals,[207, 211] thereby inhibiting the development of scaling.

■ ENVIRONMENTAL IMPLICATIONS AND RESEARCH OUTLOOK

As we have discussed the formation, transport mechanisms, and fouling behavior of crumpled NF membranes, we further propose that the ideal crumpled morphology of polyamide film should possess 1) large surface areas (e.g., high aspect ratios of the surface roughness features) and thin thickness for improving the theoretical water permeance, 2) high interconnectivity for internal voids in the crumpled NF membranes (e.g., more optimized water transport pathways for approaching the ideal water permeance and enhanced membrane anti-fouling properties), 3) patterned or rough surface to create localized turbulence, and 4) excellent mechanical strength. To achieve this ideal/controllable morphology, a better understanding of the mechanisms of the formation of crumpled morphology is needed. Although some existing formation models shed light on the mechanisms in generating crumpled polyamide layers, it is still a long way to achieve a quantitative prediction to guide the fine-tuning of the detailed morphological features. Furthermore, since the state-of-the-art separation performance of crumpled NF membranes (mostly at bench scales) has been dramatically improved compared with the commercial counterparts (Fig. 2), subsequent efforts should focus on their long-term stability and scale-up.

To scale up the crumpled NF, defect-free membranes with large areas should be first fabricated, which need simple and controllable fabrication protocols.[212] More importantly, with these highly permeable NF membranes, researchers also need to focus on the better translation of high-performance membranes to more efficient processes. For example, a recent study[213] highlighted the high permeance NF membrane may not automatically guarantee low energy consumption, nor does a highly selective membrane guarantee better permeate water quality. Therefore, one needs to optimize the membrane module, system, and process to fully unleash the potential of crumpled NF for simultaneously achieving low energy consumption, high product water quality, and a better system flux distribution to avoid fouling issues (Fig. 7). For example, newly designed spacers and flow channels to match crumpled morphologies, multi-stage inter-pumping design or closed-circuit system,[214] and submerged NF membrane process.[215] In addition to water permeance, membrane selectivity is also very important for target pollutant removal. Even though crumpled NF membranes may exhibit enhanced selectivity for water/solute and solute/solute, further studies are still needed to improve/tailor the selectivity for specific applications.

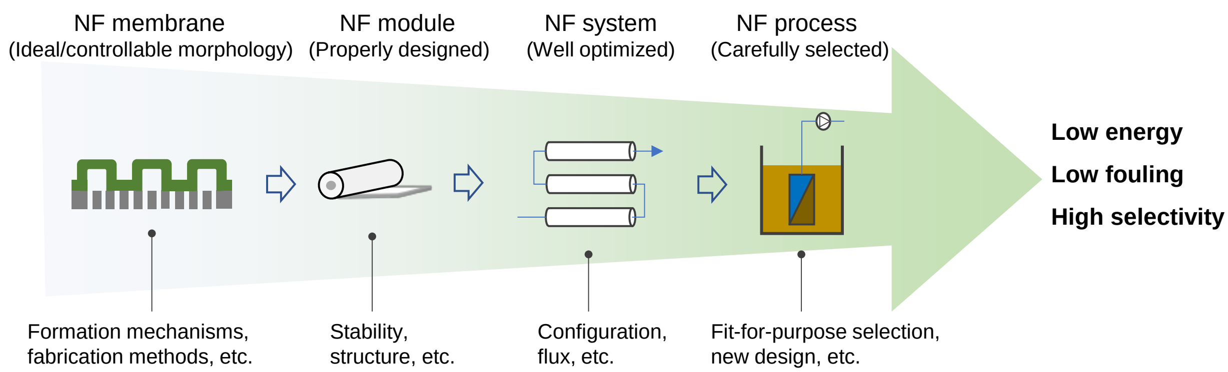

Figure 7. Schematic diagrams of outlooks and future perspectives of crumpled NF membranes. NF membranes with ideal/controllable morphologies are pursued with the better understanding of morphology formation and the development of simple and controllable fabrication protocols. Beyond membrane fabrication, researchers also need to optimize membrane modules, systems, and processes to fully unleash the potential of crumpled NF for achieving low energy consumption, low membrane fouling, and high selectivity.

ACKNOWLEDGMENT

This work was jointly supported by a grant from the Natural Science Foundation of China (52070147) and a grant from the Research Grants Council of the Hong Kong Special Administration Region, China (SRFS2021-7S04). Lu Elfa Peng is supported an RGC Postdoctoral Fellowship from the Research Grants Council of the Hong Kong Special Administration Region, China (PDFS2223-7S02).

ASSOCIATED CONTENT

Support information

Support information of this manuscript can be found online. The support information provides 1) Examples of the polyamide layers with other morphologies; 2) increases in the surface area of polyamide layers with simplified stripe and nodular morphologies; 3) classifications, fabrication methods, and separation performances of the PIP-based NF membranes with crumpled morphologies; 4) selectivity of the PIP-based NF membranes with crumpled morphologies; 5) topographical features of the morphologies; and 6) separation performances of several commercial PIP-based NF membranes.

■ REFERENCES

1. Boussu, K.; Van der Bruggen, B.; Volodin, A.; Van Haesendonck, C.; Delcour, J. A.; Van der Meeren, P.; Vandecasteele, C., Characterization of commercial nanofiltration membranes and comparison with self-made polyethersulfone membranes. *Desalination* **2006,** *191* (1), 245-253.
2. Mohammad, A. W.; Teow, Y. H.; Ang, W. L.; Chung, Y. T.; Oatley-Radcliffe, D. L.; Hilal, N., Nanofiltration membranes review: Recent advances and future prospects. *Desalination* **2015,** *356*, 226-254.
3. Hao Guo, X. L., Wulin Yang, Zhikan Yao, Ying Mei, Lu Elfa Peng, Zhe Yang, Senlin Shao, Chuyang Y. Tang, Nanofiltration for drinking water treatment: a review. *Front. Chem. Sci. Eng.* **2022,** *16* (5), 1-18.
4. Tang, C. Y.; Yang, Z.; Guo, H.; Wen, J. J.; Nghiem, L. D.; Cornelissen, E., Potable Water Reuse through Advanced Membrane Technology. *Environ. Sci. Technol.* **2018,** *52* (18), 10215-10223.
5. Shannon, M. A.; Bohn, P. W.; Elimelech, M.; Georgiadis, J. G.; Marinas, B. J.; Mayes, A. M., Science and technology for water purification in the coming decades. *Nature* **2008,** *452* (7185), 301-310.
6. Elimelech, M.; Phillip, W. A., The future of seawater desalination: energy, technology, and the environment. *Science* **2011,** *333* (6043), 712-717.
7. Salehi, F., Current and future applications for nanofiltration technology in the food processing. *Food and Bioproducts Processing* **2014,** *92* (2), 161-177.
8. Marchetti, P.; Jimenez Solomon, M. F.; Szekely, G.; Livingston, A. G., Molecular Separation with Organic Solvent Nanofiltration: A Critical Review. *Chemical Reviews* **2014,** *114* (21), 10735-10806.
9. Yang, Z.; Sun, P.-F.; Li, X.; Gan, B.; Wang, L.; Song, X.; Park, H.-D.; Tang, C. Y., A Critical Review on Thin-Film Nanocomposite Membranes with Interlayered Structure: Mechanisms, Recent Developments, and Environmental Applications. *Environ. Sci. Technol.* **2020,** *54* (24), 15563-15583.

10. Werber, J. R.; Deshmukh, A.; Elimelech, M., The critical need for increased selectivity, not increased water permeability, for desalination membranes. *Environ. Sci. Technol. Lett.* **2016,** *3* (4), 112-120.

11. Park, H. B.; Kamcev, J.; Robeson, L. M.; Elimelech, M.; Freeman, B. D., Maximizing the right stuff: The trade-off between membrane permeability and selectivity. *Science* **2017,** *356* (6343).

12. Ritt, C. L.; Stassin, T.; Davenport, D. M.; DuChanois, R. M.; Nulens, I.; Yang, Z.; Ben-Zvi, A.; Segev-Mark, N.; Elimelech, M.; Tang, C. Y.; Ramon, G. Z.; Vankelecom, I. F. J.; Verbeke, R., The open membrane database: Synthesis–structure–performance relationships of reverse osmosis membranes. *J. Membr. Sci.* **2022,** *641*, 119927.

13. Yang, Z.; Guo, H.; Tang, C. Y., The upper bound of thin-film composite (TFC) polyamide membranes for desalination. *J. Membr. Sci.* **2019,** *590*, 117297.

14. Yang, Z.; Long, L.; Wu, C.; Tang, C. Y., High Permeance or High Selectivity? Optimization of System-Scale Nanofiltration Performance Constrained by the Upper Bound. *ACS ES&T Engineering* **2022,** *2* (3), 377-390.

15. Lu, X.; Elimelech, M., Fabrication of desalination membranes by interfacial polymerization: History, current efforts, and future directions. *Chemical Society Reviews* **2021,** *50* (11), 6290-6307.

16. Werber, J. R.; Osuji, C. O.; Elimelech, M., Materials for next-generation desalination and water purification membranes. *Nature Reviews Materials* **2016**, 16018.

17. Petersen, R. J., Composite reverse osmosis and nanofiltration membranes. *J. Membr. Sci.* **1993,** *83* (1), 81-150.

18. Culp, T. E.; Khara, B.; Brickey, K. P.; Geitner, M.; Zimudzi, T. J.; Wilbur, J. D.; Jons, S. D.; Roy, A.; Paul, M.; Ganapathysubramanian, B.; Zydney, A. L.; Kumar, M.; Gomez, E. D., Nanoscale control of internal inhomogeneity enhances water transport in desalination membranes. *Science* **2021,** *371* (6524), 72-75.

19. Freger, V.; Ramon, G. Z., Polyamide desalination membranes: Formation, structure, and properties. *Prog. Polym. Sci.* **2021,** *122*, 101451.

20. Song, X.; Gan, B.; Qi, S.; Guo, H.; Tang, C. Y.; Zhou, Y.; Gao, C., Intrinsic Nanoscale Structure of Thin Film Composite Polyamide Membranes: Connectivity, Defects, and Structure–Property Correlation. *Environ. Sci. Technol.* **2020,** *54* (6), 3559-3569.

21. Lin, L.; Lopez, R.; Ramon, G. Z.; Coronell, O., Investigating the void structure of the polyamide active layers of thin-film composite membranes. *J. Membr. Sci.* **2016,** *497*, 365-376.

22. Pacheco, F.; Sougrat, R.; Reinhard, M.; Leckie, J. O.; Pinnau, I., 3D visualization of the internal nanostructure of polyamide thin films in RO membranes. *J. Membr. Sci.* **2016,** *501*, 33-44.

23. Bason, S.; Oren, Y.; Freger, V., Characterization of ion transport in thin films using electrochemical impedance spectroscopy: II: Examination of the polyamide layer of RO membranes. *J. Membr. Sci.* **2007,** *302* (1), 10-19.

24. Song, X.; Smith, J. W.; Kim, J.; Zaluzec, N. J.; Chen, W.; An, H.; Dennison, J. M.; Cahill, D. G.; Kulzick, M. A.; Chen, Q., Unraveling the Morphology–Function Relationships of Polyamide Membranes Using Quantitative Electron Tomography. *ACS Applied Materials & Interfaces* **2019,** *11* (8), 8517-8526.

25. Mi, B.; Coronell, O.; Mariñas, B. J.; Watanabe, F.; Cahill, D. G.; Petrov, I., Physico-chemical characterization of NF/RO membrane active layers by Rutherford backscattering spectrometry. *J. Membr. Sci.* **2006,** *282* (1), 71-81.

26. Peng, L. E.; Yang, Z.; Long, L.; Zhou, S.; Guo, H.; Tang, C. Y., A critical review on porous substrates of TFC polyamide membranes: Mechanisms, membrane performances, and future perspectives. *J. Membr. Sci.* **2022,** *641*, 119871.

27. Mondal, S.; Griffiths, I. M.; Ramon, G. Z., Forefronts in structure–performance models of

separation membranes. *J. Membr. Sci.* **2019,** *588*, 117166.

28. Peng, L. E.; Gan, Q.; Yang, Z.; Wang, L.; Sun, P.-F.; Guo, H.; Park, H.-D.; Tang, C. Y., Deciphering the Role of Amine Concentration on Polyamide Formation toward Enhanced RO Performance. *ACS ES&T Engineering* **2022,** *2* (5), 903-912.

29. Tan, Z.; Chen, S.; Peng, X.; Zhang, L.; Gao, C., Polyamide membranes with nanoscale turing structures for water purification. *Science* **2018,** *360* (6388), 518-521.

30. Pacheco, F. A.; Pinnau, I.; Reinhard, M.; Leckie, J. O., Characterization of isolated polyamide thin films of RO and NF membranes using novel TEM techniques. *J. Membr. Sci.* **2010,** *358* (1-2), 51-59.

31. Cheng, X.; Lai, C.; Li, J.; Zhou, W.; Zhu, X.; Wang, Z.; Ding, J.; Zhang, X.; Wu, D.; Liang, H.; Zhao, C., Toward Enhancing Desalination and Heavy Metal Removal of TFC Nanofiltration Membranes: A Cost-Effective Interface Temperature-Regulated Interfacial Polymerization. *ACS Applied Materials & Interfaces* **2021,** *13* (48), 57998-58010.

32. Sun, Z.; Wu, Q.; Ye, C.; Wang, W.; Zheng, L.; Dong, F.; Yi, Z.; Xue, L.; Gao, C., Nanovoid membranes embedded with hollow zwitterionic nanocapsules for a superior desalination performance. *Nano Lett.* **2019,** *19* (5), 2953-2959.

33. Yuan, B.; Zhao, S.; Hu, P.; Cui, J.; Niu, Q. J., Asymmetric polyamide nanofilms with highly ordered nanovoids for water purification. *Nat. Commun.* **2020,** *11* (1), 6102.

34. Liang, Y.; Zhu, Y.; Liu, C.; Lee, K.-R.; Hung, W.-S.; Wang, Z.; Li, Y.; Elimelech, M.; Jin, J.; Lin, S., Polyamide nanofiltration membrane with highly uniform sub-nanometre pores for sub-1 Å precision separation. *Nat. Commun.* **2020,** *11* (1), 2015.

35. Wang, F.; Zheng, T.; Wang, P.; Chen, M.; Wang, Z.; Jiang, H.; Ma, J., Enhanced Water Permeability and Antifouling Property of Coffee-Ring-Textured Polyamide Membranes by In Situ Incorporation of a Zwitterionic Metal-Organic Framework. *Environ. Sci. Technol.* **2021,** *55* (8), 5324-5334.

36. Mansourpanah, Y.; Ghanbari, A.; Yazdani, H.; Mohammadi, A. G.; Rahimpour, A., Silver-polyamidoamine/graphene oxide thin film nanofiltration membrane with improved antifouling and antibacterial properties for water purification and desalination. *Desalination* **2021,** *511*.

37. Ren, Y.; Zhu, J.; Cong, S.; Wang, J.; Van der Bruggen, B.; Liu, J.; Zhang, Y., High flux thin film nanocomposite membranes based on porous organic polymers for nanofiltration. *J. Membr. Sci.* **2019,** *585*, 19-28.

38. Wang, Z.; Zhu, X.; Cheng, X.; Bai, L.; Luo, X.; Xu, D.; Ding, J.; Wang, J.; Li, G.; Shao, P.; Liang, H., Nanofiltration Membranes with Octopus Arm-Sucker Surface Morphology: Filtration Performance and Mechanism Investigation. *Environ. Sci. Technol.* **2021**.

39. Wang, Z.; Zhu, X.; Cheng, X.; Bai, L.; Luo, X.; Xu, D.; Ding, J.; Wang, J.; Li, G.; Shao, P.; Liang, H., Nanofiltration Membranes with Octopus Arm-Sucker Surface Morphology: Filtration Performance and Mechanism Investigation. *Environ. Sci. Technol.* **2021,** *55* (24), 16676-16686.

40. Gao, L.; Wang, H.; Zhang, Y.; Wang, M., Nanofiltration membrane characterization and application: extracting lithium in lepidolite leaching solution. *Membranes* **2020,** *10* (8), 178.

41. Zheng, J.; Li, M.; Yu, K.; Hu, J.; Zhang, X.; Wang, L., Sulfonated multiwall carbon nanotubes assisted thin-film nanocomposite membrane with enhanced water flux and anti-fouling property. *J. Membr. Sci.* **2017,** *524*, 344-353.

42. Tang, Y.; Zhang, L.; Shan, C.; Xu, L.; Yu, L.; Gao, H., Enhancing the permeance and antifouling properties of thin-film composite nanofiltration membranes modified with hydrophilic capsaicin-mimic moieties. *J. Membr. Sci.* **2020,** *610*.

43. Hao, Y.; Li, Q.; He, B.; Liao, B.; Li, X.; Hu, M.; Ji, Y.; Cui, Z.; Younas, M.; Li, J., An ultrahighly permeable-selective nanofiltration membrane mediated by an in situ formed interlayer. *J. Mater. Chem. A* **2020,** *8* (10), 5275-5283.

44. Zhang, N.; Song, X.; Chen, Y.; Jiang, B.; Zhang, L.; Jiang, H., A facile and economic route assisted by trace tannic acid to construct a high-performance thin film composite NF membrane for desalination. *Environmental Science: Water Research & Technology* **2021,** *7* (5), 956-968.

45. Lai, G. S.; Lau, W. J.; Goh, P. S.; Ismail, A. F.; Tan, Y. H.; Chong, C. Y.; Krause-Rehberg, R.; Awad, S., Tailor-made thin film nanocomposite membrane incorporated with graphene oxide using novel interfacial polymerization technique for enhanced water separation. *Chemical Engineering Journal* **2018,** *344*, 524-534.

46. Hu, R.; He, Y.; Zhang, C.; Zhang, R.; Li, J.; Zhu, H., Graphene oxide-embedded polyamide nanofiltration membranes for selective ion separation. *J. Mater. Chem. A* **2017,** *5* (48), 25632-25640.

47. Song, Q.; Lin, Y.; Ueda, T.; Istirokhatun, T.; Shen, Q.; Guan, K.; Yoshioka, T.; Matsuyama, H., Mechanism insights into the role of the support mineralization layer toward ultrathin polyamide nanofilms for ultrafast molecular separation. *J. Mater. Chem. A* **2021,** *9* (46), 26159-26171.

48. Zhu, X.; Yang, Z.; Gan, Z.; Cheng, X.; Tang, X.; Luo, X.; Xu, D.; Li, G.; Liang, H., Toward tailoring nanofiltration performance of thin-film composite membranes: Novel insights into the role of poly(vinyl alcohol) coating positions. *J. Membr. Sci.* **2020,** *614*.

49. Teng, X.; Fang, W.; Liang, Y.; Lin, S.; Lin, H.; Liu, S.; Wang, Z.; Zhu, Y.; Jin, J., High-performance polyamide nanofiltration membrane with arch-bridge structure on a highly hydrated cellulose nanofiber support. *Science China Materials* **2020**.

50. Han, S.; Mai, Z.; Wang, Z.; Zhang, X.; Zhu, J.; Shen, J.; Wang, J.; Wang, Y.; Zhang, Y., Covalent Organic Framework-Mediated Thin-Film Composite Polyamide Membranes toward Precise Ion Sieving. *ACS Applied Materials & Interfaces* **2022,** *14* (2), 3427-3436.

51. Safarpour, M.; Vatanpour, V.; Khataee, A.; Esmaeili, M., Development of a novel high flux and fouling-resistant thin film composite nanofiltration membrane by embedding reduced graphene oxide/TiO2. *Sep. Purif. Technol.* **2015,** *154*, 96-107.

52. Asad, A.; Aktij, S. A.; Karami, P.; Sameoto, D.; Sadrzadeh, M., Micropatterned Thin-Film Composite Poly(piperazine-amide) Nanofiltration Membranes for Wastewater Treatment. *ACS Applied Polymer Materials* **2021,** *3* (12), 6653-6665.

53. Zhang, Z.; Shi, X.; Wang, R.; Xiao, A.; Wang, Y., Ultra-permeable polyamide membranes harvested by covalent organic framework nanofiber scaffolds: a two-in-one strategy. *Chem. Sci.* **2019,** *10* (39), 9077-9083.

54. Wang, Z.; Wang, Z.; Lin, S.; Jin, H.; Gao, S.; Zhu, Y.; Jin, J., Nanoparticle-templated nanofiltration membranes for ultrahigh performance desalination. *Nat. Commun.* **2018,** *9* (1), 2004.

55. Jiang, C.; Tian, L.; Zhai, Z.; Shen, Y.; Dong, W.; He, M.; Hou, Y.; Niu, Q. J., Thin-film composite membranes with aqueous template-induced surface nanostructures for enhanced nanofiltration. *J. Membr. Sci.* **2019,** *589*, 117244.

56. Eckert, K.; Acker, M.; Tadmouri, R.; Pimienta, V., Chemo-Marangoni convection driven by an interfacial reaction: Pattern formation and kinetics. *Chaos: An Interdisciplinary Journal of Nonlinear Science* **2012,** *22* (3), 037112.

57. Qin, D.; Huang, G.; Terada, D.; Jiang, H.; Ito, M. M.; H. Gibbons, A.; Igarashi, R.; Yamaguchi, D.; Shirakawa, M.; Sivaniah, E.; Ghalei, B., Nanodiamond mediated interfacial polymerization for high performance nanofiltration membrane. *J. Membr. Sci.* **2020,** *603*.

58. Weinman, S. T.; Fierce, E. M.; Husson, S. M., Nanopatterning commercial nanofiltration and reverse osmosis membranes. *Sep. Purif. Technol.* **2019,** *209*, 646-657.

59. Lin, L.; Feng, C.; Lopez, R.; Coronell, O., Identifying facile and accurate methods to measure the thickness of the active layers of thin-film composite membranes – A comparison of seven characterization techniques. *J. Membr. Sci.* **2016,** *498*, 167-179.

60. Freger, V., Swelling and Morphology of the Skin Layer of Polyamide Composite Membranes: An

Atomic Force Microscopy Study. *Environ. Sci. Technol.* **2004,** *38* (11), 3168-3175.

61. Zhu, C.-Y.; Liu, C.; Yang, J.; Guo, B.-B.; Li, H.-N.; Xu, Z.-K., Polyamide nanofilms with linearly-tunable thickness for high performance nanofiltration. *J. Membr. Sci.* **2021,** *627*.

62. Misdan, N.; Lau, W. J.; Ismail, A. F.; Matsuura, T., Formation of thin film composite nanofiltration membrane: Effect of polysulfone substrate characteristics. *Desalination* **2013,** *329*, 9-18.

63. Barambu, N. U.; Bilad, M. R.; Wibisono, Y.; Jaafar, J.; Mahlia, T. M. I.; Khan, A. L., Membrane surface patterning as a fouling mitigation strategy in liquid filtration: A review. *Polymers* **2019,** *11* (10), 1687.

64. Heinz, O.; Aghajani, M.; Greenberg, A. R.; Ding, Y., Surface-patterning of polymeric membranes: fabrication and performance. *Current Opinion in Chemical Engineering* **2018,** *20*, 1-12.

65. Ding, Y.; Maruf, S.; Aghajani, M.; Greenberg, A. R., Surface patterning of polymeric membranes and its effect on antifouling characteristics. *Separation Science and Technology* **2017,** *52* (2), 240-257.

66. Won, Y.-J.; Lee, J.; Choi, D.-C.; Chae, H. R.; Kim, I.; Lee, C.-H.; Kim, I.-C., Preparation and Application of Patterned Membranes for Wastewater Treatment. *Environ. Sci. Technol.* **2012,** *46* (20), 11021-11027.

67. Ilyas, A.; Yihdego Gebreyohannes, A.; Qian, J.; Reynaerts, D.; Kuhn, S.; Vankelecom, I. F. J., Micro-patterned membranes prepared via modified phase inversion: Effect of modified interface on water fluxes and organic fouling. *J. Colloid Interface Sci.* **2021,** *585*, 490-504.

68. Weinman, S. T.; Husson, S. M., Influence of chemical coating combined with nanopatterning on alginate fouling during nanofiltration. *J. Membr. Sci.* **2016,** *513*, 146-154.

69. Malakian, A.; Zhou, Z.; Messick, L.; Spitzer, T. N.; Ladner, D. A.; Husson, S. M., Understanding the Role of Pattern Geometry on Nanofiltration Threshold Flux. *Membranes* **2020,** *10* (12), 445.

70. Mazinani, S.; Al-Shimmery, A.; Chew, Y. M. J.; Mattia, D., 3D Printed Fouling-Resistant Composite Membranes. *ACS Applied Materials & Interfaces* **2019,** *11* (29), 26373-26383.

71. Lyu, Z.; Ng, T. C. A.; Tran-Duc, T.; Lim, G. J. H.; Gu, Q.; Zhang, L.; Zhang, Z.; Ding, J.; Phan-Thien, N.; Wang, J.; Ng, H. Y., 3D-printed surface-patterned ceramic membrane with enhanced performance in crossflow filtration. *J. Membr. Sci.* **2020,** *606*, 118138.

72. Maruf, S. H.; Greenberg, A. R.; Ding, Y., Influence of substrate processing and interfacial polymerization conditions on the surface topography and permselective properties of surface-patterned thin-film composite membranes. *J. Membr. Sci.* **2016,** *512*, 50-60.

73. Gençal, Y.; Durmaz, E. N.; Çulfaz-Emecen, P. Z., Preparation of patterned microfiltration membranes and their performance in crossflow yeast filtration. *J. Membr. Sci.* **2015,** *476*, 224-233.

74. Choi, W.; Chan, E. P.; Park, J.-H.; Ahn, W.-G.; Jung, H. W.; Hong, S.; Lee, J. S.; Han, J.-Y.; Park, S.; Ko, D.-H.; Lee, J.-H., Nanoscale Pillar-Enhanced Tribological Surfaces as Antifouling Membranes. *ACS Applied Materials & Interfaces* **2016,** *8* (45), 31433-31441.

75. Choi, D.-C.; Jung, S.-Y.; Won, Y.-J.; Jang, J. H.; Lee, J.-W.; Chae, H.-R.; Lim, J.; Ahn, K. H.; Lee, S.; Kim, J.-H.; Park, P.-K.; Lee, C.-H., Effect of Pattern Shape on the Initial Deposition of Particles in the Aqueous Phase on Patterned Membranes during Crossflow Filtration. *Environ. Sci. Technol. Lett.* **2017,** *4* (2), 66-70.

76. Zhu, X.; Tang, X.; Luo, X.; Yang, Z.; Cheng, X.; Gan, Z.; Xu, D.; Li, G.; Liang, H., Stainless steel mesh supported thin-film composite nanofiltration membranes for enhanced permeability and regeneration potential. *J. Membr. Sci.* **2021,** *618*.

77. Liu, K.; Liu, N.; Ma, S.; Cheng, P.; Hu, W.; Jia, X.; Cheng, Q.; Xu, J.; Guo, Q.; Wang, D., Highly Permeable Polyamide Nanofiltration Membrane Mediated by an Upscalable Wet-Laid EVOH Nanofibrous Scaffold. *ACS Applied Materials & Interfaces* **2021,** *13* (19), 23142-23152.

78. Gui, L.; Dong, J.; Fang, W.; Zhang, S.; Zhou, K.; Zhu, Y.; Zhang, Y.; Jin, J., Ultrafast Ion Sieving from Honeycomb-like Polyamide Membranes Formed Using Porous Protein Assemblies. *Nano Lett.* **2020**.

79. Peng, L. E.; Yao, Z.; Yang, Z.; Guo, H.; Tang, C. Y., Dissecting the Role of Substrate on the Morphology and Separation Properties of Thin Film Composite Polyamide Membranes: Seeing Is Believing. *Environ. Sci. Technol.* **2020,** *54* (11), 6978-6986.

80. Wu, M.-B.; Lv, Y.; Yang, H.-C.; Liu, L.-F.; Zhang, X.; Xu, Z.-K., Thin film composite membranes combining carbon nanotube intermediate layer and microfiltration support for high nanofiltration performances. *J. Membr. Sci.* **2016,** *515*, 238-244.

81. Choi, W.; Lee, C.; Yoo, C. H.; Shin, M. G.; Lee, G. W.; Kim, T.-S.; Jung, H. W.; Lee, J. S.; Lee, J.-H., Structural tailoring of sharkskin-mimetic patterned reverse osmosis membranes for optimizing biofouling resistance. *J. Membr. Sci.* **2020,** *595*, 117602.

82. Dai, R.; Wang, X.; Tang, C. Y.; Wang, Z., Dually Charged MOF-Based Thin-Film Nanocomposite Nanofiltration Membrane for Enhanced Removal of Charged Pharmaceutically Active Compounds. *Environ. Sci. Technol.* **2020,** *54* (12), 7619-7628.

83. Xu, D.; Zhu, X.; Luo, X.; Guo, Y.; Liu, Y.; Yang, L.; Tang, X.; Li, G.; Liang, H., MXene Nanosheet Templated Nanofiltration Membranes toward Ultrahigh Water Transport. *Environ. Sci. Technol.* **2021,** *55* (2), 1270-1278.

84. Gao, X.; Li, P.; Gu, Z.; Xiao, Q.; Yu, S.; Hou, L. a., Preparation of poly(piperazine-amide) nanofilms with micro-wrinkled surface via nanoparticle-templated interfacial polymerization: Performance and mechanism. *J. Membr. Sci.* **2021,** *638*.

85. Zhu, J.; Hou, J.; Yuan, S.; Zhao, Y.; Li, Y.; Zhang, R.; Tian, M.; Li, J.; Wang, J.; Van der Bruggen, B., MOF-positioned polyamide membranes with a fishnet-like structure for elevated nanofiltration performance. *J. Mater. Chem. A* **2019,** *7* (27), 16313-16322.

86. Wu, M.; Ma, T.; Su, Y.; Wu, H.; You, X.; Jiang, Z.; Kasher, R., Fabrication of composite nanofiltration membrane by incorporating attapulgite nanorods during interfacial polymerization for high water flux and antifouling property. *J. Membr. Sci.* **2017,** *544*, 79-87.

87. Kong, G.; Fan, L.; Zhao, L.; Feng, Y.; Cui, X.; Pang, J.; Guo, H.; Sun, H.; Kang, Z.; Sun, D.; Mintova, S., Spray-dispersion of ultra-small EMT zeolite crystals in thin-film composite membrane for high-permeability nanofiltration process. *J. Membr. Sci.* **2021,** *622*, 119045.

88. Lee, T. H.; Park, I.; Oh, J. Y.; Jang, J. K.; Park, H. B., Facile Preparation of Polyamide Thin-Film Nanocomposite Membranes Using Spray-Assisted Nanofiller Predeposition. *Ind. Eng. Chem. Res* **2019,** *58* (10), 4248-4256.

89. Yang, Z.; Wu, Y.; Wang, J.; Cao, B.; Tang, C. Y., In Situ Reduction of Silver by Polydopamine: A Novel Antimicrobial Modification of a Thin-Film Composite Polyamide Membrane. *Environ. Sci. Technol.* **2016,** *50* (17), 9543-50.

90. Zhang, Q.; Fan, L.; Yang, Z.; Zhang, R.; Liu, Y.-n.; He, M.; Su, Y.; Jiang, Z., Loose nanofiltration membrane for dye/salt separation through interfacial polymerization with in-situ generated TiO2 nanoparticles. *Applied Surface Science* **2017,** *410*, 494-504.

91. Wu, X.; Yang, L.; Meng, F.; Shao, W.; Liu, X.; Li, M., ZIF-8-incorporated thin-film nanocomposite (TFN) nanofiltration membranes: Importance of particle deposition methods on structure and performance. *J. Membr. Sci.* **2021,** *632*.

92. Istirokhatun, T.; Lin, Y.; Wang, S.; Shen, Q.; Segawa, J.; Guan, K.; Matsuyama, H., Novel thin-film composite membrane with ultrathin surface mineralization layer engineered by electrostatic attraction induced In-situ assembling process for high-performance nanofiltration. *Chemical Engineering Journal* **2021,** *417*.

93. Yang, Z.; Guo, H.; Yao, Z.-k.; Mei, Y.; Tang, C. Y., Hydrophilic Silver Nanoparticles Induce

Selective Nanochannels in Thin Film Nanocomposite Polyamide Membranes. *Environ. Sci. Technol.* **2019,** *53* (9), 5301-5308.

94. Yin, J.; Yang, Z.; Tang, C. Y.; Deng, B., Probing the Contributions of Interior and Exterior Channels of Nanofillers toward the Enhanced Separation Performance of a Thin-Film Nanocomposite Reverse Osmosis Membrane. *Environ. Sci. Technol. Lett.* **2020,** *7* (10), 766-772.

95. Li, J.; Liu, R.; Zhu, J.; Li, X.; Yuan, S.; Tian, M.; Wang, J.; Luis, P.; der Bruggen, B. V.; Lin, J., Electrophoretic nuclei assembly of MOFs in polyamide membranes for enhanced nanofiltration. *Desalination* **2021,** *512*.

96. Khan, N. A.; Yuan, J.; Wu, H.; Huang, T.; You, X.; Rahman, A. U.; Azad, C. S.; Olson, M. A.; Jiang, Z., Covalent Organic Framework Nanosheets as Reactive Fillers To Fabricate Free-Standing Polyamide Membranes for Efficient Desalination. *ACS Applied Materials & Interfaces* **2020,** *12* (24), 27777-27785.

97. Xu, H.; Feng, W.; Sheng, M.; Yuan, Y.; Wang, B.; Wang, J.; Wang, Z., Covalent organic frameworks-incorporated thin film composite membranes prepared by interfacial polymerization for efficient CO2 separation. *Chinese Journal of Chemical Engineering* **2022,** *43*, 152-160.

98. Dong, L.-x.; Huang, X.-c.; Wang, Z.; Yang, Z.; Wang, X.-m.; Tang, C. Y., A thin-film nanocomposite nanofiltration membrane prepared on a support with in situ embedded zeolite nanoparticles. *Sep. Purif. Technol.* **2016,** *166*, 230-239.

99. Borjigin, B.; Liu, l.; Yu, L.; Xu, L.; Zhao, C.; Wang, J., Influence of incorporating beta zeolite nanoparticles on water permeability and ion selectivity of polyamide nanofiltration membranes. *Journal of Environmental Sciences* **2020,** *98*, 77-84.

100. Han, S.; Wang, Z.; Cong, S.; Zhu, J.; Zhang, X.; Zhang, Y., Root-like polyamide membranes with fast water transport for high-performance nanofiltration. *J. Mater. Chem. A* **2020,** *8* (47), 25028-25034.

101. Lu, Y.; Wang, R.; Zhu, Y.; Wang, Z.; Fang, W.; Lin, S.; Jin, J., Two-dimensional fractal nanocrystals templating for substantial performance enhancement of polyamide nanofiltration membrane. *Proc. Natl. Acad. Sci.* **2021,** *118* (37).

102. Liu, Z.; Wang, T.; Wang, D.; Mi, Z., Regulating the morphology of nanofiltration membrane by thermally induced inorganic salt crystals for efficient water purification. *J. Membr. Sci.* **2021,** *617*.

103. Yang, Z.; Huang, X.; Ma, X.-h.; Zhou, Z.-w.; Guo, H.; Yao, Z.; Feng, S.-P.; Tang, C. Y., Fabrication of a novel and green thin-film composite membrane containing nanovoids for water purification. *J. Membr. Sci.* **2019,** *570-571*, 314-321.

104. Liang, Y.; Teng, X.; Chen, R.; Zhu, Y.; Jin, J.; Lin, S., Polyamide Nanofiltration Membranes from Emulsion-Mediated Interfacial Polymerization. *ACS ES&T Engineering* **2021,** *1* (3), 533-542.

105. Zhu, X.; Cheng, X.; Luo, X.; Liu, Y.; Xu, D.; Tang, X.; Gan, Z.; Yang, L.; Li, G.; Liang, H., Ultrathin thin-film composite polyamide membranes constructed on hydrophilic poly(vinyl alcohol) decorated support toward enhanced nanofiltration performance. *Environ. Sci. Technol.* **2020,** *54* (10), 6365-6374.

106. Bai, L.; Liu, Y.; Bossa, N.; Ding, A.; Ren, N.; Li, G.; Liang, H.; Wiesner, M. R., Incorporation of cellulose nanocrystals (CNCs) into the polyamide layer of thin-film composite (TFC) nanofiltration membranes for enhanced separation performance and antifouling properties. *Environ. Sci. Technol.* **2018,** *52* (19), 11178-11187.

107. Wang, Z.; Liang, S.; Kang, Y.; Zhao, W.; Xia, Y.; Yang, J.; Wang, H.; Zhang, X., Manipulating interfacial polymerization for polymeric nanofilms of composite separation membranes. *Prog. Polym. Sci.* **2021,** *122*, 101450.

108. Rodriguez-Hernandez, J., Wrinkled interfaces: Taking advantage of surface instabilities to pattern polymer surfaces. *Prog. Polym. Sci.* **2015,** *42*, 1-41.

109. Kondo, S.; Miura, T., Reaction-Diffusion Model as a Framework for Understanding Biological Pattern Formation. *Science* **2010,** *329* (5999), 1616-1620.

110. Landge, A. N.; Jordan, B. M.; Diego, X.; Müller, P., Pattern formation mechanisms of self-organizing reaction-diffusion systems. *Developmental Biology* **2020,** *460* (1), 2-11.

111. Li, B.; Japip, S.; Chung, T.-S., Molecularly tunable thin-film nanocomposite membranes with enhanced molecular sieving for organic solvent forward osmosis. *Nat. Commun.* **2020,** *11* (1), 1198.

112. Oertel, H., *Prandtl's essentials of fluid mechanics*. Springer: 2004.

113. Ma, X.-H.; Yao, Z.-K.; Yang, Z.; Guo, H.; Xu, Z.-L.; Tang, C. Y.; Elimelech, M., Nanofoaming of Polyamide Desalination Membranes To Tune Permeability and Selectivity. *Environ. Sci. Technol. Lett.* **2018,** *5* (2), 123-130.

114. Peng, L. E.; Yao, Z.; Liu, X.; Deng, B.; Guo, H.; Tang, C. Y., Tailoring Polyamide Rejection Layer with Aqueous Carbonate Chemistry for Enhanced Membrane Separation: Mechanistic Insights, Chemistry-Structure-Property Relationship, and Environmental Implications. *Environ. Sci. Technol.* **2019,** *53* (16), 9764-9770.

115. Song, X.; Gan, B.; Yang, Z.; Tang, C. Y.; Gao, C., Confined nanobubbles shape the surface roughness structures of thin film composite polyamide desalination membranes. *J. Membr. Sci.* **2019,** *582*, 342-349.

116. Gan, Q.; Peng, L. E.; Guo, H.; Yang, Z.; Tang, C. Y., Cosolvent-Assisted Interfacial Polymerization toward Regulating the Morphology and Performance of Polyamide Reverse Osmosis Membranes: Increased m-Phenylenediamine Solubility or Enhanced Interfacial Vaporization? *Environ. Sci. Technol.* **2022,** *56* (14), 10308-10316.

117. Zhu, X.; Tang, X.; Luo, X.; Cheng, X.; Xu, D.; Gan, Z.; Wang, W.; Bai, L.; Li, G.; Liang, H., Toward enhancing the separation and antifouling performance of thin-film composite nanofiltration membranes: A novel carbonate-based preoccupation strategy. *J. Colloid Interface Sci.* **2020,** *571*, 155-165.

118. Liu, S.; Wu, C.; Hung, W.-S.; Lu, X.; Lee, K.-R., One-step constructed ultrathin Janus polyamide nanofilms with opposite charges for highly efficient nanofiltration. *J. Mater. Chem. A* **2017,** *5* (44), 22988-22996.

119. He, Y.; Liu, J.; Han, G.; Chung, T.-S., Novel thin-film composite nanofiltration membranes consisting of a zwitterionic co-polymer for selenium and arsenic removal. *J. Membr. Sci.* **2018,** *555*, 299-306.

120. Shen, L.; Cheng, R.; Yi, M.; Hung, W.-S.; Japip, S.; Tian, L.; Zhang, X.; Jiang, S.; Li, S.; Wang, Y., Polyamide-based membranes with structural homogeneity for ultrafast molecular sieving. *Nat. Commun.* **2022,** *13* (1), 500.

121. Zhang, X.; Yang, W.; Wang, Q.; Huang, F.; Gao, C.; Xue, L., Tuning the nano-porosity and nano-morphology of nano-filtration (NF) membranes: Divalent metal nitrates modulated inter-facial polymerization. *J. Membr. Sci.* **2021,** *640*.

122. Wu, B.; Wang, N.; Lei, J.-H.; Shen, Y.; An, Q.-F., Intensification of mass transfer for zwitterionic amine monomers in interfacial polymerization to fabricate monovalent salt/antibiotics separation membrane. *J. Membr. Sci.* **2022,** *643*, 120050.

123. Wang, M.; Stafford, C. M.; Cox, L. M.; Blevins, A. K.; Aghajani, M.; Killgore, J. P.; Ding, Y., Controlled Growth of Polyamide Films atop Homogenous and Heterogeneous Hydrogels using Gel-Liquid Interfacial Polymerization. *Macromol Chem Phys* **2019,** *220*.

124. Ghosh, A. K.; Hoek, E. M., Impacts of support membrane structure and chemistry on polyamide–polysulfone interfacial composite membranes. *J. Membr. Sci.* **2009,** *336* (1-2), 140-148.

125. Yao, Z.; Guo, H.; Yang, Z.; Qing, W.; Tang, C. Y., Preparation of nanocavity-contained thin film composite nanofiltration membranes with enhanced permeability and divalent to monovalent ion

selectivity. *Desalination* **2018,** *445*, 115-122.

126. Ji, X.; Li, G.; Chen, G.; Qian, Y.; Jin, H.; Yao, Z.; Zhang, L., Aminated substrate based thin film composite nanofiltration membrane with high separation performance by chemically inhibiting the intrusion of polyamide. *Desalination* **2022,** *532*, 115724.

127. Pan, K.; Gu, H.; Cao, B., Interfacially polymerized thin-film composite membrane on UV-induced surface hydrophilic-modified polypropylene support for nanofiltration. *Polymer Bulletin* **2014,** *71* (2), 415-431.

128. Yao, Z.; Guo, H.; Yang, Z.; Lin, C.; Zhu, B.; Dong, Y.; Tang, C. Y., Reactable substrate participating interfacial polymerization for thin film composite membranes with enhanced salt rejection performance. *Desalination* **2018,** *436*, 1-7.

129. Zhu, J.; Qin, L.; Uliana, A.; Hou, J.; Wang, J.; Zhang, Y.; Li, X.; Yuan, S.; Li, J.; Tian, M.; Lin, J.; Van der Bruggen, B., Elevated performance of thin film nanocomposite membranes enabled by modified hydrophilic MOFs for nanofiltration. *ACS Applied Materials & Interfaces* **2017,** *9* (2), 1975-1986.

130. Chen, X.; Wang, W.; Zhu, L.; Liu, C.; Cui, F.; Li, N.; Zhang, B., Graphene Oxide/Polyamide-Based Nanofiltration Membranes for Water Purification. *ACS Applied Nano Materials* **2020,** *4* (1), 673-682.

131. Xu, S.; Li, S.; Guo, X.; Huang, H.; Qiao, Z.; Zhong, C., Co-assembly of soluble metal–organic polyhedrons for high-flux thin-film nanocomposite membranes. *J. Colloid Interface Sci.* **2022,** *615*, 10-18.

132. Sun, F.; Zeng, H.; Tao, S.; Huang, Y.; Dong, W.; Xing, D. Y., Nanofiltration membrane fabrication by the introduction of polyhedral oligomeric silsesquioxane nanoparticles: Feasibility evaluation and the mechanisms for breaking “trade-off” effect. *Desalination* **2022,** *527*, 115515.

133. Zhan, Z.-M.; Xu, Z.-L.; Zhu, K.-K.; Xue, S.-M.; Ji, C.-H.; Huang, B.-Q.; Tang, C. Y.; Tang, Y.-J., Superior nanofiltration membranes with gradient cross-linked selective layer fabricated via controlled hydrolysis. *J. Membr. Sci.* **2020,** *604*.

134. Zhan, Z.-M.; Xu, Z.-L.; Zhu, K.-K.; Tang, Y.-J., How to understand the effects of heat curing conditions on the morphology and performance of polypiperazine-amide NF membrane. *J. Membr. Sci.* **2020,** *597*, 117640.

135. Zhan, Z.-M.; Zhang, X.; Fang, Y.-X.; Tang, Y.-J.; Zhu, K.-K.; Ma, X.-H.; Xu, Z.-L., Polyamide Nanofiltration Membranes with Enhanced Desalination and Antifouling Performance Enabled by Surface Grafting Polyquaternium-7. *Ind. Eng. Chem. Res* **2021,** *60* (39), 14297-14306.

136. Huang, B.-Q.; Tang, Y.-J.; Gao, A.-R.; Zeng, Z.-X.; Xue, S.-M.; Ji, C.-H.; Tang, C. Y.; Xu, Z.-L., Dually charged polyamide nanofiltration membranes fabricated by microwave-assisted grafting for heavy metals removal. *J. Membr. Sci.* **2021,** *640*.

137. Huang, B. Q.; Tang, Y. J.; Zeng, Z. X.; Xue, S. M.; Ji, C. H.; Xu, Z. L., High-Performance Zwitterionic Nanofiltration Membranes Fabricated via Microwave-Assisted Grafting of Betaine. *ACS Applied Materials & Interfaces* **2020,** *12* (31), 35523-35531.

138. Zhu, X.; Xu, D.; Gan, Z.; Luo, X.; Tang, X.; Cheng, X.; Bai, L.; Li, G.; Liang, H., Improving chlorine resistance and separation performance of thin-film composite nanofiltration membranes with in-situ grafted melamine. *Desalination* **2020,** *489*.

139. Chiao, Y. H.; Patra, T.; Ang, M.; Chen, S. T.; Almodovar, J.; Qian, X.; Wickramasinghe, R.; Hung, W. S.; Huang, S. H.; Chang, Y.; Lai, J. Y., Zwitterion Co-Polymer PEI-SBMA Nanofiltration Membrane Modified by Fast Second Interfacial Polymerization. *Polymers (Basel)* **2020,** *12* (2).

140. Shang, C.; Wang, L.; Xia, J.; Zhang, S., Macropatterning of Microcrumpled Nanofiltration Membranes by Spacer Imprinting for Low-Scaling Desalination. *Environ. Sci. Technol.* **2020,** *54* (23), 15527-15533.

141. Malakian, A.; Husson, S. M., Understanding the roles of patterning and foulant chemistry on nanofiltration threshold flux. *J. Membr. Sci.* **2020,** *597*, 117746.

142. Jiang, C.; Zhang, L.; Li, P.; Sun, H.; Hou, Y.; Niu, Q. J., Ultrathin Film Composite Membranes Fabricated by Novel In Situ Free Interfacial Polymerization for Desalination. *ACS Applied Materials & Interfaces* **2020,** *12* (22), 25304-25315.

143. Wu, Q.; Zhang, S.; Zuo, X.; Liu, L.; Xiong, J.; He, J.; Zhou, Y.; Ma, C.; Chen, Z.; Yu, S., Preparation and characterization of CeO2@high silica ZSM-5 inorganic-organic hybrid polyamide nanofiltration membrane. *J. Membr. Sci.* **2022,** *641*.

144. Wang, Y.; Wang, T.; Li, S.; Zhao, Z.; Zheng, X.; Zhang, L.; Zhao, Z., Novel Poly(piperazinamide)/poly(m-phenylene isophthalamide) composite nanofiltration membrane with polydopamine coated silica as an interlayer for the splendid performance. *Sep. Purif. Technol.* **2022,** *285*, 120390.

145. Lan, H.; Zhai, Y.; Chen, K.; Zhai, Z.; Jiang, C.; Li, P.; Hou, Y.; Jason Niu, Q., Fabrication of high performance nanofiltration membrane by construction of Noria based nanoparticles interlayer. *Sep. Purif. Technol.* **2022,** *290*, 120781.

146. Zhu, X.; Zhang, X.; Li, J.; Luo, X.; Xu, D.; Wu, D.; Wang, W.; Cheng, X.; Li, G.; Liang, H., Crumple-textured polyamide membranes via MXene nanosheet-regulated interfacial polymerization for enhanced nanofiltration performance. *J. Membr. Sci.* **2021,** *635*.

147. Zhao, S.; Li, L.; Wang, M.; Tao, L.; Hou, Y.; Niu, Q. J., Rapid in-situ covalent crosslinking to construct a novel azo-based interlayer for high-performance nanofiltration membrane. *Sep. Purif. Technol.* **2021,** *258*.

148. You, X.; Xiao, K.; Wu, H.; Li, Y.; Li, R.; Yuan, J.; Zhang, R.; Zhang, Z.; Liang, X.; Shen, J.; Jiang, Z., Electrostatic-modulated interfacial polymerization toward ultra-permselective nanofiltration membranes. *iScience* **2021,** *24* (4), 102369.

149. Yang, Z.; Li, L.; Jiang, C.; Zhao, N.; Zhang, S.; Guo, Y.; Chen, Y.; Xue, S.; Ji, C.; Zhao, S.; Gonzales, R. R.; Matsuyama, H.; Xia, J.; Niu, Q. J., Tailored thin film nanocomposite membrane incorporated with Noria for simultaneously overcoming the permeability-selectivity trade-off and the membrane fouling in nanofiltration process. *J. Membr. Sci.* **2021,** *640*.

150. Lonsdale, H.; Riley, R.; Lyons, C.; Carosella, D., Transport in composite reverse osmosis membranes. In *Membrane Processes in Industry and Biomedicine*, Springer: 1971; pp 101-122.

151. Long, L.; Wu, C.; Yang, Z.; Tang, C. Y., Carbon Nanotube Interlayer Enhances Water Permeance and Antifouling Performance of Nanofiltration Membranes: Mechanisms and Experimental Evidence. *Environ. Sci. Technol.* **2022,** *56* (4), 2656-2664.

152. Wang, F.; Yang, Z.; Tang, C. Y., Modelling water transport in interlayered thin-film nanocomposite membranes: gutter effect vs. funnel effect. *ACS ES&T Engineering* **2022**, in press.

153. Ramon, G. Z.; Wong, M. C.; Hoek, E. M., Transport through composite membrane, part 1: Is there an optimal support membrane? *J. Membr. Sci.* **2012,** *415*, 298-305.

154. Wijmans, J.; Hao, P., Influence of the porous support on diffusion in composite membranes. *J. Membr. Sci.* **2015,** *494*, 78-85.

155. Kattula, M.; Ponnuru, K.; Zhu, L.; Jia, W.; Lin, H.; Furlani, E. P., Designing ultrathin film composite membranes: The impact of a gutter layer. *Scientific reports* **2015,** *5* (1), 1-9.

156. Ramon, G. Z.; Hoek, E. M. V., Transport through composite membranes, part 2: Impacts of roughness on permeability and fouling. *J. Membr. Sci.* **2013,** *425-426*, 141-148.

157. Zhai, Z.; Jiang, C.; Zhao, N.; Dong, W.; Lan, H.; Wang, M.; Niu, Q. J., Fabrication of advanced nanofiltration membranes with nanostrand hybrid morphology mediated by ultrafast Noria–polyethyleneimine codeposition. *J. Mater. Chem. A* **2018,** *6* (42), 21207-21215.

158. Hu, R.; Zhang, R.; He, Y.; Zhao, G.; Zhu, H., Graphene oxide-in-polymer nanofiltration

membranes with enhanced permeability by interfacial polymerization. *J. Membr. Sci.* **2018,** *564*, 813-819.

159. Casanova, S.; Liu, T.-Y.; Chew, Y.-M. J.; Livingston, A.; Mattia, D., High flux thin-film nanocomposites with embedded boron nitride nanotubes for nanofiltration. *J. Membr. Sci.* **2020,** *597*.

160. Ormanci-Acar, T.; Tas, C. E.; Keskin, B.; Ozbulut, E. B. S.; Turken, T.; Imer, D.; Tufekci, N.; Menceloglu, Y. Z.; Unal, S.; Koyuncu, I., Thin-film composite nanofiltration membranes with high flux and dye rejection fabricated from disulfonated diamine monomer. *J. Membr. Sci.* **2020,** *608*.

161. Zhang, R.; Zhu, Y.; Zhang, L.; Lu, Y.; Yang, Z.; Zhang, Y.; Jin, J., Polyamide Nanofiltration Membranes from Surfactant‐Assembly Regulated Interfacial Polymerization: The Effect of Alkyl Chain. *Macromolecular Chemistry and Physics* **2021,** *222* (20).

162. Yang, S.; Jiang, Q.; Zhang, K., Few-layers 2D O–MoS2 TFN nanofiltration membranes for future desalination. *J. Membr. Sci.* **2020,** *604*, 118052.

163. Yang, Z.; Wu, Y.; Guo, H.; Ma, X.-H.; Lin, C.-E.; Zhou, Y.; Cao, B.; Zhu, B.-K.; Shih, K.; Tang, C. Y., A novel thin-film nano-templated composite membrane with in situ silver nanoparticles loading: Separation performance enhancement and implications. *J. Membr. Sci.* **2017,** *544*, 351-358.

164. Xu, S.; Lin, H.; Li, G.; Wang, J.; Han, Q.; Liu, F., Anionic covalent organic framework as an interlayer to fabricate negatively charged polyamide composite nanofiltration membrane featuring ions sieving. *Chemical Engineering Journal* **2022,** *427*.

165. Xia, D.; Zhang, M.; Tong, C.; Wang, Z.; Liu, H.; Zhu, L., In-situ incorporating zwitterionic nanocellulose into polyamide nanofiltration membrane towards excellent perm-selectivity and antifouling performances. *Desalination* **2022,** *521*.

166. Wang, Y.; Xu, H.; Ding, M.; Zhang, L.; Chen, G.; Fu, J.; Wang, A.; Chen, J.; Liu, B.; Yang, W., MXene-regulation polyamide membrane featuring with bubble-like nodule for efficient dye/salt separation and antifouling performance. *RSC Advances* **2022,** *12* (17), 10267-10279.

167. Ji, C.; Lin, C.-W.; Zhang, S.; Guo, Y.; Yang, Z.; Hu, W.; Xue, S.; Niu, Q. J.; Kaner, R. B., Ultrapermeable nanofiltration membranes with tunable selectivity fabricated with polyaniline nanofibers. *J. Mater. Chem. A* **2022,** *10* (8), 4392-4401.

168. Lin, B.; Tan, H.; Liu, W.; Gao, C.; Pan, Q., Preparation of a novel zwitterionic striped surface thin-film composite nanofiltration membrane with excellent salt separation performance and antifouling property. *RSC Advances* **2020,** *10* (27), 16168-16178.

169. Shang, W.; Sun, F.; Jia, W.; Guo, J.; Yin, S.; Wong, P. W.; An, A. K., High-performance nanofiltration membrane structured with enhanced stripe nano-morphology. *J. Membr. Sci.* **2020,** *600*, 117852.

170. Maruf, S. H.; Greenberg, A. R.; Pellegrino, J.; Ding, Y., Fabrication and characterization of a surface-patterned thin film composite membrane. *J. Membr. Sci.* **2014,** *452*, 11-19.

171. ElSherbiny, I. M. A.; Khalil, A. S. G.; Ulbricht, M., Surface micro-patterning as a promising platform towards novel polyamide thin-film composite membranes of superior performance. *J. Membr. Sci.* **2017,** *529*, 11-22.

172. Zhou, Z.; Ling, B.; Battiato, I.; Husson, S. M.; Ladner, D. A., Concentration polarization over reverse osmosis membranes with engineered surface features. *J. Membr. Sci.* **2021,** *617*, 118199.

173. Li, H.; Shi, W.; Zhang, Y.; Du, Q.; Qin, X.; Su, Y., Improved performance of poly(piperazine amide) composite nanofiltration membranes by adding aluminum hydroxide nanospheres. *Sep. Purif. Technol.* **2016,** *166*, 240-251.

174. Yang, W.; Zhu, Y.; Sun, Z.; Gao, C.; Xue, L., Self‐Sealed Polyamide (PA)/Zinc Imidazole Framework (ZIF) Thin Film Nanocomposite (TFN) Nanofiltration Membranes with Nanoscale Turing Type Structures. *Advanced Materials Interfaces* **2019,** *6* (22).

175. Al-Amoudi, A.; Lovitt, R. W., Fouling strategies and the cleaning system of NF membranes and

factors affecting cleaning efficiency. *J. Membr. Sci.* **2007,** *303* (1), 4-28.

176. Shao, S.; Fu, W.; Li, X.; Shi, D.; Jiang, Y.; Li, J.; Gong, T.; Li, X., Membrane fouling by the aggregations formed from oppositely charged organic foulants. *Water Res.* **2019,** *159*, 95-101.

177. Shao, S.; Li, Y.; Jin, T.; Liu, W.; Shi, D.; Wang, J.; Wang, Y.; Jiang, Y.; Li, J.; Li, H., Biofouling layer maintains low hydraulic resistances and high ammonia removal in the UF process operated at low flux. *J. Membr. Sci.* **2020,** *596*, 117612.

178. Tang, C. Y.; Chong, T. H.; Fane, A. G., Colloidal interactions and fouling of NF and RO membranes: A review. *Advances in Colloid and Interface Science* **2011,** *164* (1–2), 126-143.

179. Shang, C.; Pranantyo, D.; Zhang, S., Understanding the Roughness–Fouling Relationship in Reverse Osmosis: Mechanism and Implications. *Environ. Sci. Technol.* **2020,** *54* (8), 5288-5296.

180. Vrijenhoek, E. M.; Hong, S.; Elimelech, M., Influence of membrane surface properties on initial rate of colloidal fouling of reverse osmosis and nanofiltration membranes. *J. Membr. Sci.* **2001,** *188* (1), 115-128.

181. Zhu, X.; Elimelech, M., Colloidal Fouling of Reverse Osmosis Membranes: Measurements and Fouling Mechanisms. *Environ. Sci. Technol.* **1997,** *31* (12), 3654-3662.

182. Hoek, E. M.; Bhattacharjee, S.; Elimelech, M., Effect of membrane surface roughness on colloid− membrane DLVO interactions. *Langmuir* **2003,** *19* (11), 4836-4847.

183. Richard Bowen, W.; Doneva, T. A., Atomic Force Microscopy Studies of Membranes: Effect of Surface Roughness on Double-Layer Interactions and Particle Adhesion. *J. Colloid Interface Sci.* **2000,** *229* (2), 544-549.

184. Jang, J. H.; Lee, J.; Jung, S.-Y.; Choi, D.-C.; Won, Y.-J.; Ahn, K. H.; Park, P.-K.; Lee, C.-H., Correlation between particle deposition and the size ratio of particles to patterns in nano- and micro-patterned membrane filtration systems. *Sep. Purif. Technol.* **2015,** *156*, 608-616.

185. Whitehead, K. A.; Verran, J., The Effect of Surface Topography on the Retention of Microorganisms. *Food and Bioproducts Processing* **2006,** *84* (4), 253-259.

186. Jiang, Z.; Karan, S.; Livingston, A. G., Membrane Fouling: Does Microscale Roughness Matter? *Ind. Eng. Chem. Res* **2020,** *59* (12), 5424-5431.

187. An, R.; Dong, Y.; Zhu, J.; Rao, C., Adhesion and friction forces in biofouling attachments to nanotube- and PEG- patterned TiO2 surfaces. *Colloids and Surfaces B: Biointerfaces* **2017,** *159*, 108-117.

188. Kim, T.; Kwon, S.; Lee, J.; Lee, J. S.; Kang, S., A metallic anti-biofouling surface with a hierarchical topography containing nanostructures on curved micro-riblets. *Microsystems & Nanoengineering* **2022,** *8* (1), 6.

189. Lin, W.; Zhang, Y.; Li, D.; Wang, X.-m.; Huang, X., Roles and performance enhancement of feed spacer in spiral wound membrane modules for water treatment: A 20-year review on research evolvement. *Water Res.* **2021,** *198*, 117146.

190. Du, X.; Wang, Y.; Leslie, G.; Li, G.; Liang, H., Shear stress in a pressure-driven membrane system and its impact on membrane fouling from a hydrodynamic condition perspective: a review. *Journal of Chemical Technology & Biotechnology* **2017,** *92* (3), 463-478.

191. Maruf, S. H.; Wang, L.; Greenberg, A. R.; Pellegrino, J.; Ding, Y., Use of nanoimprinted surface patterns to mitigate colloidal deposition on ultrafiltration membranes. *J. Membr. Sci.* **2013,** *428*, 598-607.

192. Kim, I.; Choi, D.-C.; Lee, J.; Chae, H.-R.; Hee Jang, J.; Lee, C.-H.; Park, P.-K.; Won, Y.-J., Preparation and application of patterned hollow-fiber membranes to membrane bioreactor for wastewater treatment. *J. Membr. Sci.* **2015,** *490*, 190-196.

193. Maruf, S. H.; Rickman, M.; Wang, L.; Mersch Iv, J.; Greenberg, A. R.; Pellegrino, J.; Ding, Y., Influence of sub-micron surface patterns on the deposition of model proteins during active filtration. *J. Membr. Sci.* **2013,** *444*, 420-428.

194. Lee, Y. K.; Won, Y.-J.; Yoo, J. H.; Ahn, K. H.; Lee, C.-H., Flow analysis and fouling on the patterned membrane surface. *J. Membr. Sci.* **2013,** *427*, 320-325.

195. Choi, D.-C.; Jung, S.-Y.; Won, Y.-J.; Jang, J. H.; Lee, J.; Chae, H.-R.; Ahn, K. H.; Lee, S.; Park, P.-K.; Lee, C.-H., Three-dimensional hydraulic modeling of particle deposition on the patterned isopore membrane in crossflow microfiltration. *J. Membr. Sci.* **2015,** *492*, 156-163.

196. Won, Y.-J.; Jung, S.-Y.; Jang, J.-H.; Lee, J.-W.; Chae, H.-R.; Choi, D.-C.; Hyun Ahn, K.; Lee, C.-H.; Park, P.-K., Correlation of membrane fouling with topography of patterned membranes for water treatment. *J. Membr. Sci.* **2016,** *498*, 14-19.

197. Ng, T. C. A.; Lyu, Z.; Wang, C.; Guo, S.; Poh, W.; Gu, Q.; Zhang, L.; Wang, J.; Ng, H. Y., Effect of surface-patterned topographies of ceramic membranes on the filtration of activated sludge and their interaction with different particle sizes. *J. Membr. Sci.* **2022,** *645*, 120125.

198. Zhao, Z.; Muylaert, K.; Szymczyk, A.; Vankelecom, I. F. J., Harvesting microalgal biomass using negatively charged polysulfone patterned membranes: Influence of pattern shapes and mechanism of fouling mitigation. *Water Res.* **2021,** *188*, 116530.

199. Chen, C. S.; Mrksich, M.; Huang, S.; Whitesides, G. M.; Ingber, D. E., Geometric Control of Cell Life and Death. *Science* **1997,** *276* (5317), 1425-1428.

200. Choi, W.; Lee, C.; Lee, D.; Won, Y. J.; Lee, G. W.; Shin, M. G.; Chun, B.; Kim, T.-S.; Park, H.-D.; Jung, H. W.; Lee, J. S.; Lee, J.-H., Sharkskin-mimetic desalination membranes with ultralow biofouling. *J. Mater. Chem. A* **2018,** *6* (45), 23034-23045.

201. Jamshidi Gohari, R.; Lau, W. J.; Matsuura, T.; Ismail, A. F., Effect of surface pattern formation on membrane fouling and its control in phase inversion process. *J. Membr. Sci.* **2013,** *446*, 326-331.

202. Liu, J.; Wang, Z.; Tang, C. Y.; Leckie, J. O., Modeling Dynamics of Colloidal Fouling of RO/NF Membranes with A Novel Collision-Attachment Approach. *Environ. Sci. Technol.* **2018,** *52* (3), 1471-1478.

203. Bacchin, P.; Aimar, P.; Field, R. W., Critical and sustainable fluxes: Theory, experiments and applications. *J. Membr. Sci.* **2006,** *281* (1-2), 42-69.

204. Le Clech, P.; Jefferson, B.; Chang, I. S.; Judd, S. J., Critical flux determination by the flux-step method in a submerged membrane bioreactor. *J. Membr. Sci.* **2003,** *227* (1), 81-93.

205. Cho, B. D.; Fane, A. G., Fouling transients in nominally sub-critical flux operation of a membrane bioreactor. *J. Membr. Sci.* **2002,** *209* (2), 391-403.

206. Yang, Z.; Wang, F.; Guo, H.; Peng, L. E.; Ma, X.-h.; Song, X.-x.; Wang, Z.; Tang, C. Y., Mechanistic Insights into the Role of Polydopamine Interlayer toward Improved Separation Performance of Polyamide Nanofiltration Membranes. *Environ. Sci. Technol.* **2020,** *54* (18), 11611-11621.

207. Rolf, J.; Cao, T.; Huang, X.; Boo, C.; Li, Q.; Elimelech, M., Inorganic Scaling in Membrane Desalination: Models, Mechanisms, and Characterization Methods. *Environ. Sci. Technol.* **2022,** *56* (12), 7484-7511.

208. Lin, N. H.; Cohen, Y., QCM study of mineral surface crystallization on aromatic polyamide membrane surfaces. *J. Membr. Sci.* **2011,** *379* (1), 426-433.

209. Mi, B.; Elimelech, M., Silica scaling and scaling reversibility in forward osmosis. *Desalination* **2013,** *312*, 75-81.

210. Qian, M.; Ma, J., The characteristics of heterogeneous nucleation on concave surfaces and implications for directed nucleation or surface activity by surface nanopatterning. *Journal of Crystal Growth* **2012,** *355* (1), 73-77.

211. Matin, A.; Rahman, F.; Shafi, H. Z.; Zubair, S. M., Scaling of reverse osmosis membranes used in water desalination: Phenomena, impact, and control; future directions. *Desalination* **2019,** *455*, 135-157.

212. Beuscher, U.; Kappert, E. J.; Wijmans, J. G., Membrane research beyond materials science. *J. Membr. Sci.* **2022,** *643*, 119902.

213. Yang, Z.; Long, L.; Wu, C.; Tang, C. Y., High Permeance or High Selectivity? Optimization of System-Scale Nanofiltration Performance Constrained by the Upper Bound. *ACS ES&T Engineering* **2021**.

214. Lin, S.; Elimelech, M., Staged reverse osmosis operation: Configurations, energy efficiency, and application potential. *Desalination* **2015,** *366*, 9-14.

215. Fujioka, T.; Ngo, M. T. T.; Makabe, R.; Ueyama, T.; Takeuchi, H.; Nga, T. T. V.; Bui, X.-T.; Tanaka, H., Submerged nanofiltration without pre-treatment for direct advanced drinking water treatment. *Chemosphere* **2021,** *265*, 129056.